

# 1 Labilization and diversification of pyrogenic dissolved organic matter by 2 microbes

3  
4 Aleksandar I. Goranov<sup>1,\*</sup>, Andrew S. Wozniak<sup>2</sup>, Kyle W. Bostick<sup>3,†</sup>, Andrew R. Zimmerman<sup>3</sup>, Siddhartha  
5 Mitra<sup>4</sup>, and Patrick G. Hatcher<sup>1</sup>

6  
7 <sup>1</sup>Department of Chemistry and Biochemistry, Old Dominion University, Norfolk, VA, USA

8 <sup>2</sup>School of Marine Science and Policy, College of Earth, Ocean, and Environment, University of Delaware, Lewes, DE, USA

9 <sup>3</sup>Department of Geological Sciences, University of Florida, Gainesville, FL, USA

10 <sup>4</sup>Department of Geological Sciences, East Carolina University, Greenville, NC, USA

11  
12 *Correspondence to:* Patrick G. Hatcher ([phatcher@odu.edu](mailto:phatcher@odu.edu))

## 13 14 Abstract

15  
16 With the increased occurrence of ~~forest fires~~wildfires around the world, interest in the chemistry of  
17 pyrogenic organic matter (pyOM) and its fate in the environment has increased. Upon leaching from soils by rain  
18 events, significant amounts of dissolved pyOM (pyDOM) enter the aquatic environment and interact with  
19 microbial communities that are essential for cycling organic matter within the different biogeochemical cycles.  
20 To evaluate the bio-~~reactivity~~degradability of pyDOM, aqueous extracts of laboratory-produced biochars were  
21 incubated with soil microbes and the molecular changes to the composition of pyDOM were probed using  
22 ultrahigh resolution mass spectrometry (Fourier transform – ion cyclotron resonance – mass spectrometry). Given  
23 that solar photo-degradation irradiation also significantly affects the composition ~~and reactivity~~ of pyDOM during  
24 terrigenousterrestrial-to-marine export, the effects of photochemistry were also evaluated in the context of  
25 pyDOM the bio-~~reactivity~~degradability of pyDOM.

26 Ultrahigh resolution mass spectrometry revealed that, ~~after incubation,~~ many different (both aromatic and  
27 aliphatic) compounds were bio-degraded. ~~, and n~~New labile compounds, 22 – 40 % of which were peptide-like,  
28 were bio-produced. ~~This~~These results indicated that a portion of pyDOM has been labilized into microbial  
29 biomass during the incubations. Fluorescence excitation-emission matrix spectra revealed that some fraction of  
30 these new bio-produced molecules is associated with proteinaceous fluorophores ~~from proteinaceous and/or~~  
31 autochthonous/microbial biomass origin. Two-dimensional <sup>1</sup>H-<sup>1</sup>H total correlation NMR spectroscopy identified  
32 a peptidoglycan-like backbone within the microbially produced compounds. These results are consistent with  
33 previous observations of nitrogen from peptidoglycans within the soil and ocean nitrogen cycles where remnants  
34 of bio-degraded pyDOM are expected to be observed.

35 Interestingly, the exact nature of the bio-produced organic matter was found to vary drastically among  
36 samples indicating that the used microbial consortium may produce different exudates based on the composition  
37 of the initial pyDOM. Another potential explanation for the vast diversity of molecules is that microbes only  
38 consume low molecular weight compounds, but they also produce reactive oxygen species (ROS), which initiate  
39 oxidative and recombination reactions that produce new molecules. Some of the bio-produced molecules (212 –  
40 308 molecular formulas) were identified in surface and abyssal oceanic samples and 81 – 192 of them were of  
41 molecular composition attributed to carboxyl-rich alicyclic molecules (CRAM). These results indicate that some  
42 of the pyDOM bio-degradation products have an oceanic fate and can be sequestered into the deep ocean. The  
43 observed microbially-mediated diversification of pyDOM suggests that pyDOM contributes to the observed large  
44 complexity of natural organic matter observed in riverine and oceanic systems. More broadly, our research shows

---

\* Current Address: Department of Earth and Environmental Sciences, Rensselaer Polytechnic Institute, Troy, NY, USA

† Current Address: Fugro GeoServices, 6100 Hillcroft Avenue, Houston, TX, USA

45 that pyDOM can be substrate for microbial growth and be incorporated into environmental food webs within the  
46 global carbon and nitrogen cycles.

## 50 1 Introduction

51  
52 Pyrogenic organic matter (pyOM), the carbonaceous solid residue that is left after biomass burning (e.g.,  
53 forest fires/wildfires, biochar production), has been gaining attention in recent years as an important active  
54 component of the global biogeochemical cycles. Compositionally, pyOM is mainly comprised of condensed  
55 aromatic compounds (ConAC) of various degrees of condensation and functionalization (Masiello, 2004;  
56 Schneider et al., 2010; Wagner et al., 2018; Wozniak et al., 2020). These ConAC molecules have been found in  
57 various environmental matrices such as soils and sediments (Schmidt and Noack, 2000; Skjemstad et al., 2002;  
58 Reisser et al., 2016) and atmospheric aerosols (Wozniak et al., 2008; Bao et al., 2017). In the terrestrial se  
59 environmental matrices, particularly in soils and sediments, ConAC were originally thought to be exclusively  
60 highly stable (“recalcitrant”) due to their highly-condensed character (Goldberg, 1985; Masiello and Druffel,  
61 1998). However, more and more studies report of the presence of pyrogenic molecules in different aquatic  
62 environments (Hockaday et al., 2006; Dittmar and Paeng, 2009; Roebuck et al., 2017; Wagner et al., 2017; Li et  
63 al., 2019). These studies support the estimates-proposition that pyOM can be solubilized upon rain events and be  
64 leached as riverine systems annually export large amounts of pyrogenic dissolved organic matter (pyDOM)  
65 resulting in large annual riverine fluxes of pyDOM from global riverine systems to the global-open ocean (Dittmar  
66 et al., 2012; Jaffé et al., 2013; Wang et al., 2016; Marques et al., 2017; Jones et al., 2020). During export, pyDOM  
67 is likely altered by various processes resulting in its degradation and alteration of its physico-chemical  
68 characteristics (Masiello, 2004; Coppola et al., 2019; Wagner et al., 2019). Using laboratory-prepared biochars  
69 and conservative assumptions, Bostick et al. (2018) approximated that > 86.5% of the leached pyDOM is  
70 degradable (e.g., mineralizable to CO<sub>2</sub>), which indicates that pyDOM is a very active component within the global  
71 carbon cycle, as previously suggested (Druffel, 2004; Lehmann, 2007; Riedel et al., 2016).

72 In sunlit aquatic environments, photo-degradation is the most significant sink for the ConAC fraction of  
73 pyDOM (Stubbins et al., 2012). The photochemistry of ConAC and pyDOM has been studied utilizing either  
74 laboratory-prepared pyDOM (Ward et al., 2014; Fu et al., 2016; Li et al., 2019; Bostick et al., 2020b; Goranov et  
75 al., 2020; Wang et al., 2020) or ConAC-rich natural organic matter (Stubbins et al., 2010, 2012; Wagner and  
76 Jaffé, 2015). These studies have reported that ConAC are exceptionally photo-labile and they degrade through a  
77 series of oxygenation, ring-opening, and decarboxylation reactions leading to a pool of smaller aliphatic by-  
78 products. Additionally, pyDOM photochemistry has been associated with the production of high fluxes of reactive  
79 oxygen species (ROS), important transients involved in the photo-transformation and photo-degradation of  
80 pyDOM (Fu et al., 2016; Li et al., 2019; Goranov et al., 2020; Wang et al., 2020). These studies have contributed  
81 to a better understanding of the biogeochemical cycling of pyDOM in the presence of sunlight in the environment.  
82 Microbial (biotic) pathways are another degradative pathway with high potential for altering and/or mineralizing  
83 pyDOM, but they-these pathways are far less understood.

84 Biotic reworking of organic molecules is a key mechanism for producing the diverse molecular  
85 composition of natural organic matter (Lechtenfeld et al., 2015; Hach et al., 2020). Due to the highly condensed  
86 character of pyOM, it is often regarded as bio-recalcitrant, though several studies have shown that a fraction of it  
87 (about 0.5 to 10 %) is indeed bio-degradable (Kuzyakov et al., 2009, 2014; Zimmerman, 2010; Zimmerman et  
88 al., 2011). PyOM is mainly comprised of ConAC (Bostick et al., 2018; Wozniak et al., 2020), which contributes  
89 to its low bio-degradability (Zimmerman, 2010). By contrast, pyDOM is highly heterogeneous (Wozniak et al.,  
90 2020), and in addition to ConAC, it contains numerous low molecular weight (LMW) species (e.g., acetate,  
91 methanol, formate; Bostick et al., 2018; Goranov et al., 2020) as well as various pyrogenic aliphatic compounds  
92 and inorganic nutrients (Hockaday et al., 2007; Mukherjee and Zimmerman, 2013; Goranov et al., 2020; Wozniak  
93 et al., 2020). The very-high solubility of pyDOM is imparted by the greater abundance of polar functional groups,  
94 which would also allow for greater microbial accessibility. To date, there is no study that evaluates the molecular-

95 scale bio-degradability of pyDOM. It is unknown whether and how (e.g., mechanistic pathways, kinetic rates)  
96 these different compound groups of pyDOM are bio-degraded and/or bio-transformed.

97 AdditionallyIn addition to the unexplored bio-degradability of pyDOM, there are concerns that biochar  
98 leachates of fire-derived substances may be toxic due to the presence of condensed and ligninaceous aromatics.  
99 It has been shown that cellulose- and pinewood-derived biochar water-extracts (i.e., pyDOM) of laboratory-made  
100 chareoals) inhibit the growth of cyanobacteria while pyDOM of lignin-derived biochar has no inhibitory effects  
101 (Smith et al., 2016). The toxicity of pyDOM has been mainly attributed to polysubstituted phenols present in the  
102 cellulose- and pinewood-derived above-mentioned biochars. In natural systems, however, it is likely that other  
103 pyDOM components also play a role in controlling the bio-reactivitydegradability and toxicity of pyDOM. An  
104 important very recent finding is that pyOM and pyDOM contain organochlorine compounds (both aliphatic and  
105 aromatic; Wozniak et al., 2020), which may enhance the toxicity of these pyrogenic substancespyDOM. Thus,  
106 biotic incubations of pyDOM are needed to reveal if microbial growth can be sustained in a pyDOM/ConAC-rich  
107 environments.

108 To explore these questions, we incubated aqueous biochar leachates (i.e., pyDOM) with a soil-derived  
109 microbial consortium and evaluated the compositional changes to pyDOM using numerous analytical techniques.  
110 Laboratory-produced biochars can be considered model pyrogenic substances as they are similar to what is  
111 produced during natural forest fireswildfires in the environment (Santín et al., 2017) but have not experienced  
112 environmental aging which would have impacted their physico-chemical properties (Ascough et al., 2011). We  
113 have used oak wood because most of riverine dissolved organic matter (DOM) is exported from forested  
114 catchments (Hedges et al., 1997). We, and used two pyrolysis temperatures (400 and 650 °C) representative of  
115 forest fire temperatures (Santín et al., 2015, 2016). As photochemistry has been shown to increase the bio-lability  
116 of various types of DOM (Kieber et al., 1989; Lindell et al., 1995; Wetzel et al., 1995; Benner and Biddanda,  
117 1998; Moran and Covert, 2003; Qualls and Richardson, 2003; Obernosterer and Benner, 2004; Abboudi et al.,  
118 2008; Chen and Jaffé, 2014; Antony et al., 2018), we also incubated pyDOM that had been photo-irradiated.  
119 Previous studies of these pyDOM samples showed that significant compositional and structural changes occur to  
120 pyDOM afterduring photo-irradiation, which certainly implies different bio-reactivitydegradability (Bostick et  
121 al., 2020b; Goranov et al., 2020).

122 In a parallel study of the same samples-incubations (Bostick et al., 2020a2021), we quantified the total  
123 organic carbon (TOC) loss, respired CO<sub>2</sub> quantities, as well as the changes to the bulk structural composition of  
124 pyDOM as determined by one-dimensional <sup>1</sup>H nuclear magnetic resonance (NMR) spectroscopy. Additionally,  
125 in that study, benzenepolycarboxylic acids (BPCA) molecular markers were used to quantify the changes specific  
126 to the condensed aromatic (ConAC) fraction of pyDOM. It was found that the pyDOM leachates derived from  
127 the biochars of higher pyrolysis temperature (650 °C) were less bio-degradable than those-the pyDOM leachates  
128 from the lower temperature (400 °C) leachatesbiochar. As expected, and photo-irradiation increased the bio-  
129 lability of pyDOM. Over the 96-day incubation, up to 48% of the carbon was respired to CO<sub>2</sub>. The degradation  
130 following-followed first-order kinetics, with LMW compounds (e.g., acetate, formate, methanol) being  
131 preferentially degraded. To elucidate the molecular-level changes taking place during the bio-incubation of  
132 pyDOM, and probe-assess the various molecules that are being degraded or produced by soil biota, we examined  
133 these samples usingemployed ultrahigh resolution mass spectrometry (Fourier transform – ion cyclotron  
134 resonance – mass spectrometry, FT-ICR-MS), two-dimensional NMR, and fluorescence spectroscopy. The  
135 collective results from these two studies improve our understanding of the degradative pathways of pyDOM and  
136 ConAC in the environment and allow us to better interpret observations pertaining to terrigenous/terrestrial-to-  
137 marine transfers and global cycling of organic matter.

## 139 2 Materials and Methods

### 141 2.1 Preparation of pyDOM samples

142  
143 Two biochars were prepared by heating laurel oak wood (*Quercus hemisphaerica*) under N<sub>2</sub> atmosphere  
144 at 400 and 650 °C for 3 hours. After grinding and sieving to particles of uniform size (0.25 - 2.00 mm), the

145 biochars were leached in 18.1 mΩ MilliQ laboratory-grade water (5 g in 500 mL) over 50 hours on a shaker table.  
146 The obtained pyDOM leachates, hereafter referred to as “Oak 400 Fresh” and “Oak 650 Fresh”, were filtered  
147 using 0.2 μm Millipore GSWP mixed cellulose ester filters. Physico-chemical characteristics of similarly  
148 produced solid biochars and their leachates were reported in several previous studies (Zimmerman, 2010;  
149 Mukherjee et al., 2011; Bostick et al., 2018; Wozniak et al., 2020). A fraction of each leachate was also subjected  
150 to photo-irradiation for 5 days in a custom-made solar simulator equipped with Q-Lab Corporation UV-A lamps  
151 (295 – 365 nm,  $\lambda_{\text{MAX}} = 340$  nm, 40 watt) equivalent to natural photo-irradiation of 12 days. Photo-transformation  
152 rates, structural changes, photo-irradiation apparatus design, and other relevant information ~~has~~ have been  
153 published previously (Bostick et al., ~~2020b~~ 2020; Goranov et al., 2020). Photo-irradiated pyDOM samples will be  
154 hereafter referred to as “Oak 400 Photo” and “Oak 650 Photo”. The four samples (Oak 400 Fresh, Oak 650 Fresh,  
155 Oak 400 Photo, Oak 650 Photo) were diluted to a uniform TOC concentration of 4.7 mgC·L<sup>-1</sup> prior to ~~microbial~~  
156 ~~incubation~~ inoculation.

## 157 158 **2.2 Microbial ~~I~~ncubations of pyDOM**

160 Microbial incubations ~~was~~ were performed using a soil-derived microbial consortium as an inoculum. Soil  
161 from the Austin Cary Memorial Forest (Gainesville, FL) was chosen, because this area is frequently subjected to  
162 prescribed burns (Johns, 2016), and its soil microbes likely interact with pyOM and pyDOM on a regular basis.  
163 Taxonomic details of ~~its~~ the used soil ~~microbial characteristics~~ have been published previously (Khodadad et al.,  
164 2011). The collected soil was treated to remove roots and detritus, and its water-extract was centrifuged to obtain  
165 a pellet. The pellet was then dissolved in 10 mL MilliQ laboratory-grade water to obtain an inoculate, 100 μL  
166 of which was used to spike 50 mL of each pyDOM substrate. Additionally, microbial nutrients (KH<sub>2</sub>PO<sub>4</sub> and  
167 (NH<sub>4</sub>)<sub>2</sub>SO<sub>4</sub>) were provided following Zimmerman (2010) to support a healthy growth medium. Samples were  
168 incubated in gas-sealed amber vials on a shaker table at 28 ± 5 °C for 10 days in the dark. Using a double-needle  
169 assembly, CO<sub>2</sub>-free air (Airgas, Zero) was flushed through the samples on days 0, 2, 5, and 10, which oxygenated  
170 the samples and removed dissolved inorganic carbon for its measurement (~~,~~ and is reported by Bostick et al.  
171 (~~2020a~~ 2021)). A procedural blank and control samples were prepared in the exact same way but were poisoned  
172 with HgCl<sub>2</sub> immediately following the mixing of the different components (pyDOM, inoculate, nutrients).  
173 Additionally, a solution of sucrose (0.5 g C<sub>12</sub>H<sub>22</sub>O<sub>11</sub> in 40 mL MilliQ laboratory-grade water) was also incubated  
174 in the same manner to serve as a positive control. All incubated samples were poisoned with HgCl<sub>2</sub> to terminate  
175 microbial activity before shipment to Old Dominion University (Norfolk, VA) for ~~spectroscopic and~~  
176 ~~spectrometric~~ analyses. Prior to spectroscopic analysis (see Sect. 2.3 and 2.5 below) or spectrometric analysis  
177 (see Sect. 2.4 below), samples were filtered using acid-washed 0.1 μm Teflon (PTFE) syringe filters. Further  
178 details about sample preparation can be found in the parallel study (Bostick et al., ~~2020a~~ 2021).

## 179 180 **2.3 Analysis of chromophoric and fluorophoric dissolved organic matter**

181 Chromophoric DOM (CDOM) measurements were performed on a Thermo Scientific Evolution 201  
182 ultraviolet-visible (UV-VIS) spectrophotometer operated in a double-beam mode. A matched Starna quartz  
183 cuvette with MilliQ water was used as a reference during all spectral measurements. Spectra were recorded from  
184 230 – 800 nm using a 1 nm step, 0.12 s integration time, and 500 nm/min scan speed. In addition to the double-  
185 beam referencing, the average noise in the 700-800 nm spectral region was subtracted from the spectra to correct  
186 for any instrument baseline drifts, temperature fluctuations, as well as scattering and refractive effects (Green and  
187 Blough, 1994; Helms et al., 2008). After consecutive procedural-blank corrections, the spectra (kept in decadic  
188 units) were normalized to the cuvette path length (1.0 cm) and ~~the~~ TOC content (in mgC·L<sup>-1</sup>) to convert them to  
189 specific absorbance spectra (L·mgC<sup>-1</sup>·cm<sup>-1</sup>; Weishaar et al., 2003). CDOM was quantified by integrating the  
190 spectra from 250 – 450 nm (Helms et al., 2008) and CDOM quantity is reported in L·mgC<sup>-1</sup>·cm<sup>-1</sup>·nm units.

191 Fluorophoric DOM (FDOM) measurements were performed on a Shimadzu RF-6000 spectrofluorometer  
192 operated in 3D acquisition mode. Samples were analyzed without dilution as no sample yielded absorbance at  
193 230 nm above 0.07 (Miller et al., 2010). Samples were excited from 230 – 500 nm (5 nm step) and emission was  
194



recorded over 250 – 650 nm (5 nm step) to obtain excitation-emission matrices (EEMs). Additionally, five replicate water Raman scans were acquired on MilliQ water in 2D emission mode by exciting the sample at 350 nm and fluorescence intensity was monitored over 365 – 450 nm (0.5 nm steps). All measurements were done with 5 nm slit widths of the monochromators, 600 nm/min scan speed, and in high-sensitivity mode.

EEMs were processed in MATLAB using the drEEM toolbox (version 0.4.0.) using previously published routines (Murphy et al., 2010, 2013). Briefly, using the *FDOMcorrect* function, the raw EEMs were adjusted for instrumental bias, blank-corrected using an EEM of the procedural blank, and scaled to adjust for any inner-filter effects using the raw UV-VIS spectra (Kothawala et al., 2013). This function also normalized the EEMs to Raman units (RU) after the area of the water Raman peak (peak maximum at 397 nm) had been determined by the *ramanintegrationrange* function (Murphy, 2011) on the averaged water Raman spectrum. The EEMs were then processed using the *smootheem* function to remove 1<sup>st</sup> and 2<sup>nd</sup> order Rayleigh signals and Raman scattering. EEMs are visualized and difference plots are generated using an in-house MATLAB script.

## 2.4 Fourier transform - ion cyclotron resonance - mass spectrometry (FT-ICR-MS)

Procedural blank, control, and incubated samples were loaded onto solid-phase extraction cartridges (Agilent Technologies Bond Elut PPL, 100 mg styrene divinyl copolymer) as previously described (Dittmar et al., 2008). Cartridges were eluted with methanol (Fisher Scientific, Optima LC-MS grade) and infused into an Apollo II electrospray ionization (ESI) source interfaced with a Bruker Daltonics Apex Qe FT-ICR-MS operating at 10 T and housed in the College of Sciences Major Instrumentation Cluster (COSMIC) facility at Old Dominion University (Norfolk, VA). The instrument is externally calibrated daily with a polyethylene glycol standard, and a surrogate laboratory pyDOM standard was analyzed before and after pyDOM-analyse the analytical sequence to verify for the lack of instrumental drift. Additionally, an instrumental blank of methanol was analyzed between samples to verify for the absence of sample carryover. Samples were analyzed in negative ionization mode. ESI spray voltages were optimized for each sample to assure for consistent spray currents among the-all samples. For each sample, 300 transients with a 4MWord time domain were collected, co-added, and the resultant free induction decay was zero-filled and sine-bell apodized. After fast Fourier transformation, internal calibration of the resultant mass spectra was performed using naturally abundant fatty acids, dicarboxylic acids, and compounds belonging to the CH<sub>2</sub>-homologous series as previously described (Sleighter et al., 2008). Then, using an in-house MATLAB script, salt, blank, and isotopologue (<sup>13</sup>C, <sup>37</sup>Cl) peaks were removed. Molecular formulas within ± 1 ppm error were assigned to FT-ICR-MS spectral peaks (S/N ≥ 3) using the Molecular Formula Calculator from the National High Magnetic Field Laboratory (Tallahassee, FL). Formula assignments were restricted to elemental composition of <sup>12</sup>C<sub>5-∞</sub>, <sup>1</sup>H<sub>1-∞</sub>, <sup>14</sup>N<sub>0-5</sub>, <sup>16</sup>O<sub>0-30</sub>, <sup>32</sup>S<sub>0-2</sub>, <sup>31</sup>P<sub>0-2</sub>, and <sup>35</sup>Cl<sub>0-4</sub>, and were refined using previously established rules (Stubbins et al., 2010). Any ambiguous peak assignments were refined by inclusion within homologous series (CH<sub>2</sub>, H<sub>2</sub>, COO, CH<sub>2</sub>O, O<sub>2</sub>, H<sub>2</sub>O, NH<sub>3</sub>, HCl) following Kujawinski and Behn (2006) and Koch et al. (2007). For all samples, at least 80% of the mass spectral peaks were assigned, and they accounted for at least 93% of the mass spectral magnitude.

Molecular composition was evaluated by plotting the molecular formulas on van Krevelen (vK) diagrams, scatterplots of the formulas' hydrogen-to-carbon (H/C) versus oxygen-to-carbon (O/C) ratios (Van Krevelen, 1950; Kim et al., 2003). Formulas were further categorized using the modified aromaticity index (AI<sub>MOD</sub>), a proxy for the aromatic character of the-associated molecules (Koch and Dittmar, 2006, 2016), and calculated as shown in Eq.1.

$$AI_{MOD} = \frac{1 + C - \frac{1}{2}O - S - \frac{1}{2}(N + P + H + Cl)}{C - \frac{1}{2}O - N - S - P} \quad \text{Eq. 1}$$

Formulas were classified as following: Condensed aromatic compounds (ConAC, AI<sub>MOD</sub> ≥ 0.67, number of C-atoms ≥ 15), aromatic (0.67 < AI<sub>MOD</sub> ≤ 0.50), olefinic/alicyclic (0 < AI<sub>MOD</sub> < 0.50), and aliphatic (AI<sub>MOD</sub> =

0). Additionally, N-containing formulas falling in the ranges of  $1.5 \leq H/C \leq 2$  and  $0.1 \leq O/C \leq 0.67$  were classified as peptide-like. Statistical evaluation of means using one-way analysis of variance (ANOVA) was performed in MATLAB using the “*anova1*” function, ~~which performs one-way analysis of variance (ANOVA)~~. Post-hoc Scheffé's assessments were performed using the “*multcompare*” function ~~in the same software~~. Pearson correlations were performed using the *corrcoef* function in the same software. Confidence level of 95% was used for all statistical assessments.

For the Kendrick ~~Mass-mass Defect-defect~~ (KMD) series analysis (described later in the manuscript), Kendrick ~~Mass-mass~~ (KM) was first calculated using the molecular weight of each compound (i.e., calculated mass from its molecular formula) following Eq. 2. Then, the Kendrick ~~Nominal-nominal Mass-mass~~ (KNM) was calculated as the ~~rounded~~-integer (no decimals) of the Kendrick ~~Mass-mass~~ (KM) as shown in Eq. 3. The Kendrick ~~Nominal-nominal Mass-mass~~ (KMD) is the difference between KM and KNM, i.e., the decimals (Eq. 4). This analysis was performed for oxygen (O), carbonyl (CO), and carboxyl (COO) series (S).

$$KM = \text{Molecular Weight} \times S \quad \text{Eq. 2}$$

where -S

$$= \frac{15.994914616.0000000}{15.994914616.0000000} \text{ for O series; } -\frac{27.994914628.0000000}{27.994914628.0000000} \text{ for CO series; and } \frac{43.98982924}{43.98982924}$$

$$KNM = \text{integer of KM} \quad \text{Eq. 3}$$

$$KMD = KM - KNM \quad \text{Eq. 4}$$

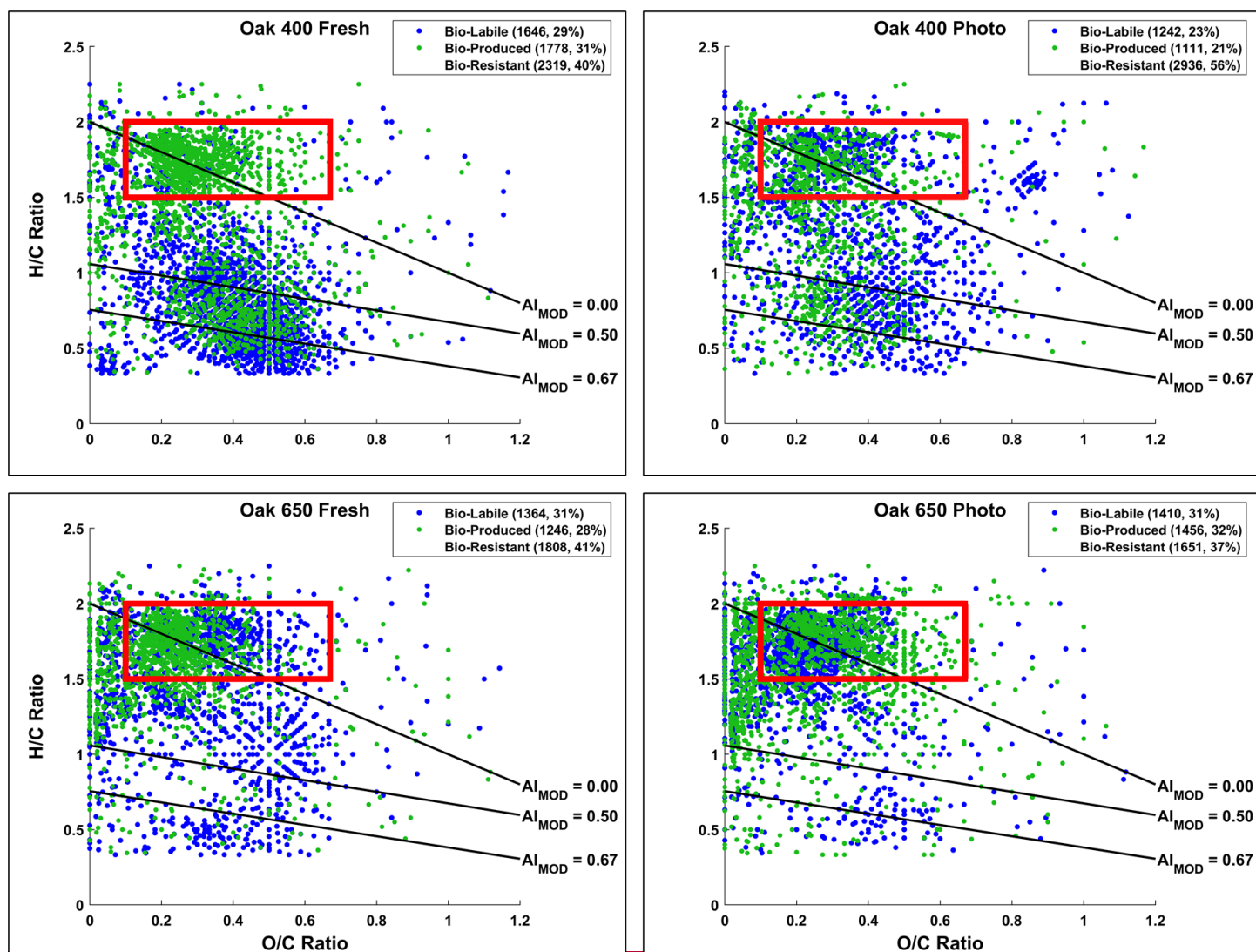
## 2.5 Two-dimensional ~~Nuclear-nuclear Magnetic-magnetic Resonance-resonance~~ (NMR) spectroscopy

One-dimensional  $^1\text{H}$  NMR spectra of the samples ~~of this project~~ were published and evaluated in the parallel study (Bostick et al., [2020a2021](#)). For the study of this manuscript, a select sample was analyzed using two-dimensional  $^1\text{H}$ - $^1\text{H}$  total correlation spectroscopy (TOCSY) to further evaluate several functional groups of interest. Analyses were performed on a 400 MHz (9.4 Tesla) Bruker BioSpin AVANCE III spectrometer fitted with a double-resonance broadband z-gradient inverse (BBI) probe in the COSMIC facility. Samples were analyzed without pre-concentration and volumetrically diluted with deuterated water ( $\text{D}_2\text{O}$ , Acros Organics, 100% D) to obtain a 90:10  $\text{H}_2\text{O}:\text{D}_2\text{O}$  solution. Further details of sample preparation and acquisition of 1D  $^1\text{H}$  spectra are published ~~elsewhere in the companion study~~ (Bostick et al., [2020a2021](#)). To obtain ultraclean NMR spectra, NMR tubes were soaked with aqua regia, rinsed extensively with ultrapure water, and individually tested as blanks to verify that no background peaks are present. While  $^1\text{H}$  spectra were originally processed using an exponential multiplication function (line broadening) of 5 Hz to obtain higher signal-to-noise for a more accurate and precise integration (Bostick et al., [2020a2021](#)), here they were re-processed using a multiplication function of 1.5 Hz to better observe the splitting (multiplicity) patterns of the peaks of interest. TOCSY spectra were acquired using the phase-sensitive gradient-enhanced *mlevgpphw5* pulse program. It utilizes a 17-step Malcolm Levitt (MLEV-17) composite scheme (Bax and Davis, 1985) for magnetization transfer between any coupled nuclear spins, and a W5-WATERGATE element for water suppression (Liu et al., 1998). Both short-range and long-range spin-spin couplings were observed using 30 ms and 100 ms mixing times, respectively. The data were then zero-filled to a 4096 x 1024 matrix and then fitted with a  $\pi/2$ -shifted (SSB = 2) sine-squared window function. Linear prediction to 256 points was used in the  $F_1$  dimension. All spectra were internally calibrated to the sharp distinguishable methanol singlet at 3.34 ppm (Gottlieb et al., 1997), and then spectra were phased and baseline-corrected.  $T_1$ -noise removal was performed by calculating the positive projection of rows with no resonances and the summed projections were subtracted from all rows in the spectrum (Klevit, 1985). The same procedure was performed for all columns ( $F_2$  dimension).

## 3 Results

### 3.1 Molecular changes to pyDOM after microbial degradation incubation

Ultrahigh resolution mass spectrometric analysis of the bio-incubated and corresponding control pyDOM leachates revealed significant changes in molecular composition after the 10-day incubation (Fig. 1). The identified molecular formulas for these samples were classified into one of three groups using a presence-absence approach (Stubbins et al., 2010; Sleighter et al., 2012). This approach identifies any common formulas among the two samples being compared (control and bio-incubated), as well as any formulas that are unique to each sample. It is important to note that the electrospray ionization (ESI) source is prone to biases, and the analytical window of FT-ICR-MS depends most critically on it. Thus, it may not identify compounds that are present if they are not ionizable (Stenson et al., 2002; Patriarca et al., 2020). Therefore, our observations are influenced by the limited analytical window, and it is essential that observations by FT-ICR-MS are always paired with supplementary quantitative techniques (optical analyses, NMR, etc.) in order to determine if the identified trends are real or an artifact of ESI charge competition (D'Andrilli et al., 2020).





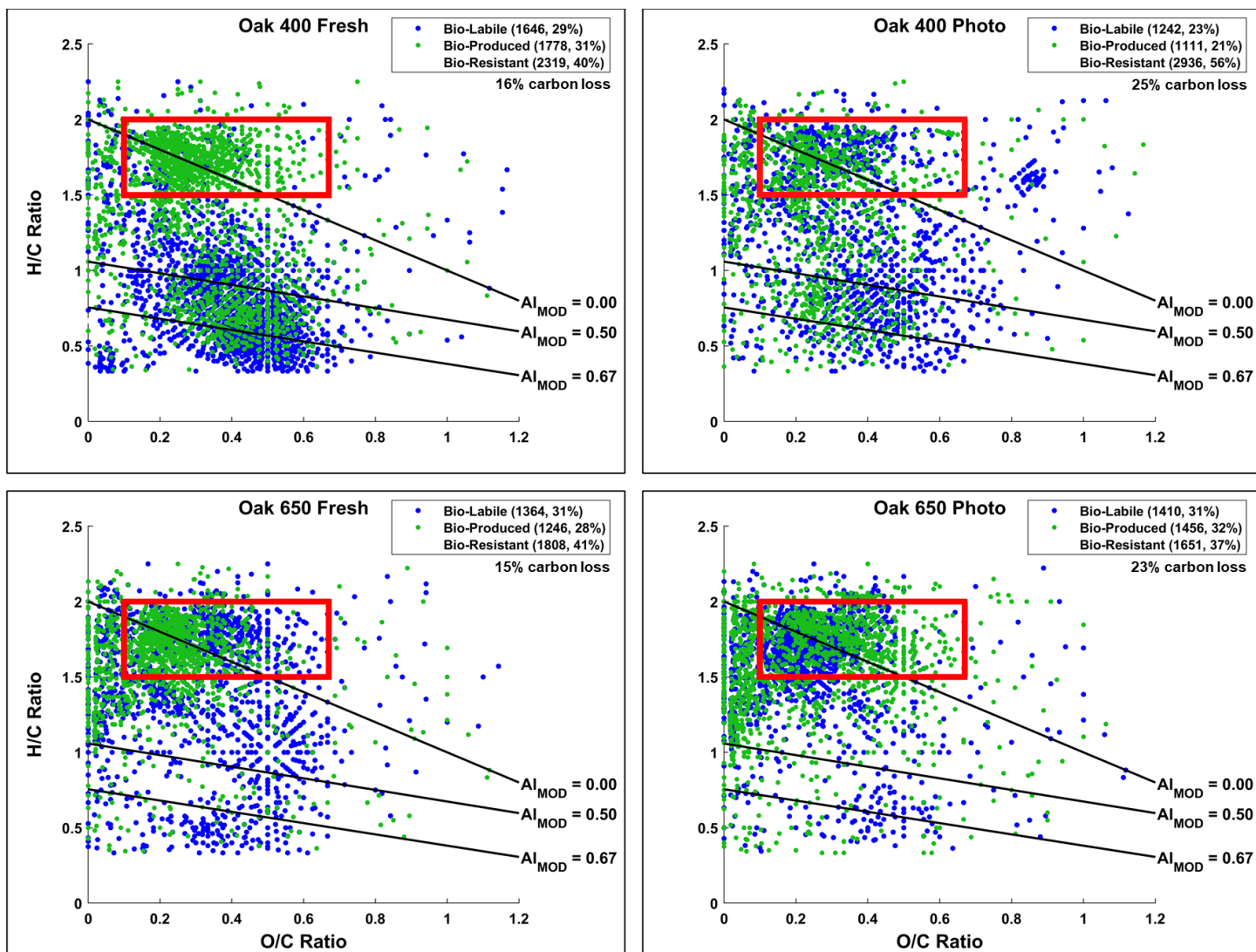


**Figure 1.** Van Krevelen (vK) diagrams of 10-day microbially incubated pyDOM leachates. Formulas are classified as **bio-labile** (molecular formulas only found in the “killed” control pyDOM leachates) and **bio-produced** (formulas that are only found in the bio-incubated samples). Formulas that are present in both the control and bio-incubated samples are operationally classified as bio-resistant and not shown for clarity. These three classes of molecules are separately plotted on vK diagrams and shown in Sect. 2 of the Supplement (Figs. S2-4). The number of formulas found in each of these pools is listed in the legends along with corresponding percentages (relative to total number of formulas in the two samples being compared). The carbon losses quantified by Bostick et al. (2021) are listed under the legends. The **black** lines indicate modified aromaticity index cutoffs (AI<sub>MOD</sub>; Koch and Dittmar, 2006, 2016), and the **red** box indicates the peptide region (valid only for N-containing formulas).

In all samples, nearly a third of the formulas (23 – 31%) present in the control samples were not observed after the biotic incubations, ~~which is~~ This is somewhat proportional to the organic carbon losses observed over the 10-day incubation by Bostick et al. (2020a,2021). The organic carbon loss was also found to be equivalent to mineralized CO<sub>2</sub> (± 4%, Bostick et al., 2021) indicating that microbial respiration had occurred though CO<sub>2</sub> mineralization can happen abiotically as well. Using the number of formulas lost as a proxy for bio-lability here, it appears that Oak 400 Fresh (1646 bio-labile formulas, 16% carbon loss) is more bio-labile than Oak 650 Fresh (1364 bio-labile formulas, 15% carbon loss). This was expected because of the richness of Oak 400 Fresh in smaller less-aromatic compounds (Wozniak et al., 2020). Upon photo-irradiation, both Oak 400 Fresh and Oak 650 Fresh experience significant changes in their molecular composition as previously described in detail by



Goranov et al. (2020). The photo-transformed pyDOM is much more aliphatic and richer in nitrogen and LMW compounds which render pyDOM to be much more biologically labile (Goranov et al., 2020). Surprisingly, it was found that Oak 400 Fresh (1646 bio-labile formulas) is more bio-labile than its photo-irradiated counterpart (Oak 400 Photo, 1242 bio-labile formulas). However, this observation using molecular data does not agree with quantitative carbon loss results for the 10-day incubation (Oak 400 Fresh: 16% carbon loss, Oak 400 Photo: 25 % carbon loss). The observed discrepancy is because LMW compounds contribute to a large fraction of the degraded carbon in the Oak 400 pyDOM systems and LMW species are not observed following the employed PPL sample preparation and FT-ICR-MS detection. A similar discrepancy is observed when comparing Oak 400 Photo (1242 bio-labile formulas, 25% carbon loss) and Oak 650 Photo (1410 bio-labile formulas, 23% carbon loss). In contrast, Oak 650 Fresh (1364 bio-labile formulas) was observed to be less bio-labile than Oak 650 Photo (1410 bio-labile formulas) via both FT-ICR-MS and the observed quantitative carbon losses (Oak 650 Fresh: 15% carbon loss, Oak 650 Photo: 23 % carbon loss). LMW species are less abundant in the Oak 650 pyDOM systems resulting in consistent trends between the analyses. Bio-degradability trends derived from FT-ICR-MS molecular data match those from the UV-VIS data from chromophoric pyDOM (Figure S1) revealing a similar inability of UV-VIS to detect LMW compounds which do not absorb UV-VIS light. In summary, we observe a degradation of a variety of different molecular classes as well as a production of many molecules that appear to be of high biological lability. However, we caution that there are observed discrepancies among carbon loss and molecular/chromophoric data for the Oak 400 pyDOM systems, an observation that highlights the need to clearly understand methodological analytical windows when interpreting molecular and spectroscopic data.

Interestingly, for all leachates, the degraded (“bio-labile”) molecules were not from a specific area of the vK diagrams but rather represent a broad range of H/C and O/C ratios and compound types (see Fig. S2). This variety of compound characteristics among bio-labile molecules suggests that the degradation pathway may not be from microbial consumption alone. It would be unlikely for the soil microorganisms to utilize organic matter compounds as food indiscriminately. Most interestingly, it is evident that large numbers of aromatic ( $AI_{MOD} \geq 0.50$ ) and some ConAC ( $AI_{MOD} \geq 0.67$ ) formulas are lost, in agreement with observed losses in CDOM (Fig. S1 in the Supplement) and losses in, as well as aryl functional groups (measured by  $^1H$  NMR) and ConAC (measured by BPCA analysis) reported in the parallel study (Bostick et al., 2020a, 2021). ConAC were found to be resistant to bio-degradation (Bostick et al., 2021) and therefore losses of specific compound classes, especially of ConAC observed via FT-ICR-MS (due to their low ionizability) might be considered an artifact due to the low ionizability of ConAC and to competition processes in the ESI source (Stenson et al., 2002; Patriarca et al., 2020). However, the agreement between FT-ICR-MS and other quantitative data (UV-VIS, NMR, TOC, BPCA) confirms the interpretation of bulk pyDOM degradation. Approximately half of the formulas (37 – 56%) in the original pyDOM leachates are classified, using the presence-absence approach, as bio-resistant (observed before and after biotic degradation). These formulas are located in all areas of the vK diagrams (Fig. S3), showing variable oxygenation and aromaticity. Furthermore, the relative peak magnitudes of these formulas did not change significantly following the incubations ( $R^2 > 0.95$ , Fig. S9; Sleighter et al., 2012), also suggesting that a wide variety of pyDOM molecules appear to be recalcitrant-resistant to microbial degradation. Using the available molecular data, it is not possible to attribute the observed recalcitrance to any molecular property. Therefore, it is likely that some of these bio-resistant molecules are still bio-labile and would have degraded in due time if the incubations were sampled at later time points. Longer biotic incubation time series should be conducted in future studies to fully differentiate between among bio-labile and bio-recalcitrant-resistant pyDOM molecules.

The use of hydrogen-to-carbon ratio (H/C) versus molecular weight (MW) plots has also been useful in interpreting ultrahigh resolution mass spectrometry data (e.g., Gonsior et al., 2018; Powers et al., 2019; Valle et al., 2020). Such graphs are presented using the presence-absence approach in Figs. S5-8 in Sect. 3 of the Supplement. These graphics help evaluate how different types of compounds (aliphatic versus aromatic) change relative to their MW. For both Oak 400 leachates, it is clear that large aromatic molecules ( $H/C < 1.5$ ,  $MW > 550$  Da) are removed during the biotic degradation, and smaller ( $300 < MW < 550$ ) aromatic compounds are produced. The consumption of large molecules indicates that microbes utilize extracellular enzymes to produce ROS which degrade larger molecules into smaller substrates (Billen et al., 1990) or secondary degradative pathways are also at play. These large aromatic molecules that are being degraded into smaller ones are mainly ligninaceous

and not ConAC, in agreement with the insignificant changes in BPCA data published by Bostick et al. (2020a,2021). With regards to the aliphatic molecules ( $H/C > 1.5$ ), it is clear that molecules of a wide range of sizes-MW are ~~removed-degraded~~ and ~~created-produced~~ during the incubations suggesting that ~~molecular weight~~MW is not a critical factor in their bio-lability. This is in apparent disagreement with the general knowledge that microbes preferentially consume ~~low molecular weight~~LMW substrates (e.g., Søndergaard and Middelboe, 1995). Bostick et al. (2021) also concluded that LMW substances are preferentially degraded in the incubations of pyDOM. The observed production of higher MW aliphatics suggest that the microbial incubations were still very active at the point of sampling (10 days). This additionally suggests that future studies need to evaluate the molecular composition of biotically incubated pyDOM over a longer time scale., which was also concluded for these samples by Bostick et al. (2020a). The consumption of large molecules indicates that microbes utilize extracellular enzymes to degrade them into smaller substrates (Billen et al., 1990) or secondary degradative pathways are also at play.

### 3.2 Composition of bio-produced organic matter

The bio-produced organic compounds can be evaluated in various ways to examine the processes that may have occurred during the incubations. Using a presence-/absence approach (Sleighter et al., 2012), the bio-produced formulas of each sample are compared with those of the other samples (Table 1). No significant overlap was found (2 – 320 formulas in common, 0 – 12%) among the molecules produced in the incubated pyDOM samples. Furthermore, no significant match was found between the bio-produced formulas of incubated pyDOM and those of the sucrose control sample (63 – 94 formulas in common, 3%, Table 1). These observations indicate that the products of the incubations were ~~either~~vastly different for each sample and ~~may-likely~~ depend on the starting substrate. An alternative explanation is that bio-produced formulas-~~or~~ were further altered post-exudation by ROS to result in their molecular diversification.

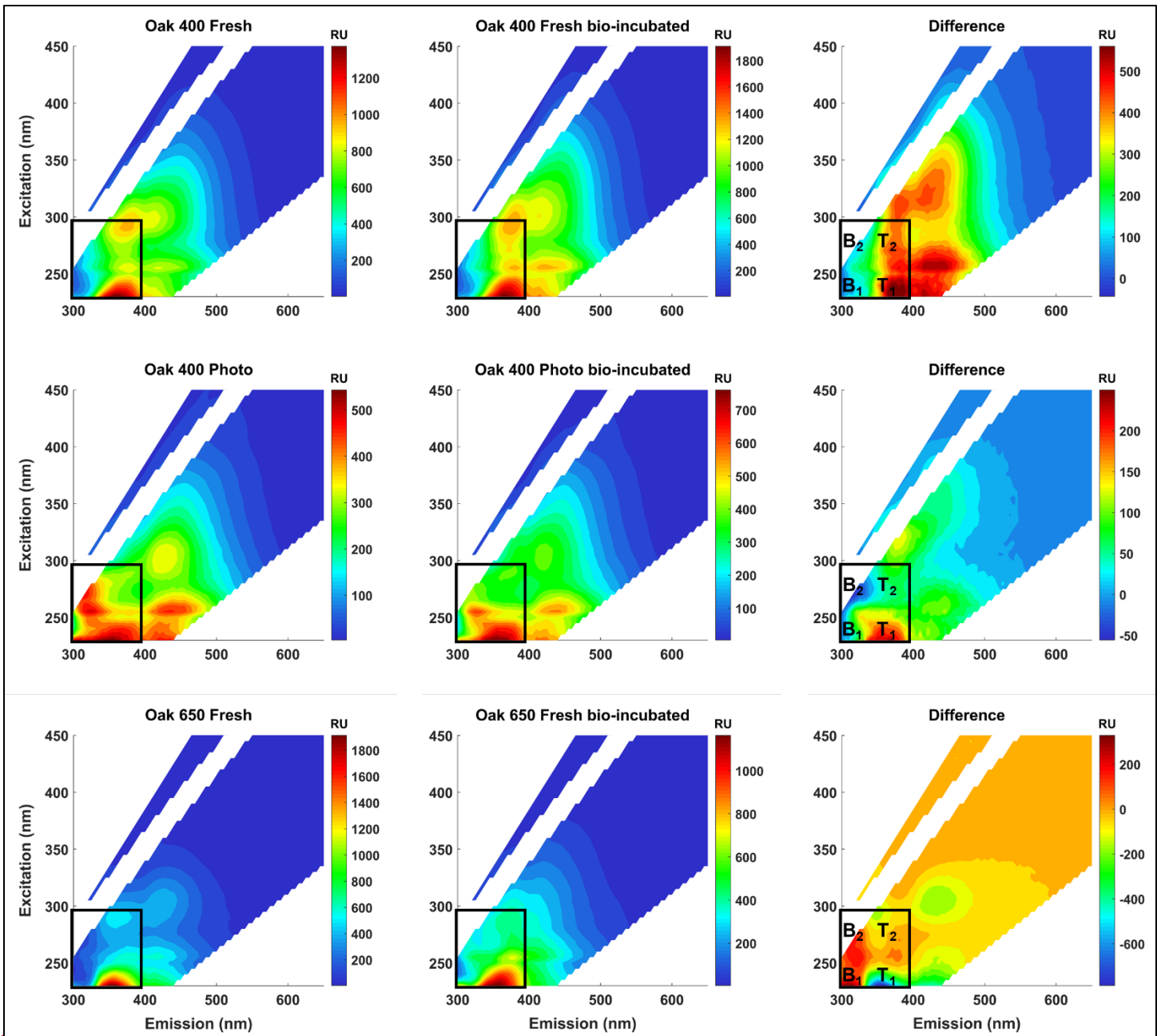
**Table 1.** Overlap of bio-produced molecular formulas among samples. The number of formulas corresponds to the formulas in common between the two samples being compared, and the percentage is relative to the total number of formulas in the two formula sets.

Sample	Oak 400 Fresh	Oak 400 Photo	Oak 650 Fresh	Oak 650 Photo
Oak 400 Fresh	-	-	-	-
Oak 400 Photo	320 (12%)	-	-	-
Oak 650 Fresh	126 (4%)	104 (5%)	-	-
Oak 650 Photo	165 (5%)	81 (3%)	2 (0%)	-
Sucrose	94 (3%)	63 (3%)	68 (3%)	83 (3%)

A significant fraction of the bio-produced organic matter was characterized as peptide-like (N-containing,  $1.5 \leq H/C \leq 2.0$ ,  $0.1 \leq O/C \leq 0.67$ ). This indicates that microbes convert a part of pyDOM into labile DOM (Moran et al., 2016; Vorobev et al., 2018), a process hereafter referred to as “microbial labilization”. Given that the pyDOM samples used in this study were poor in organic nitrogen, the microbes must have used the inorganic nitrogen ( $NH_4^+$ ) that was provided as a nutrient and converted some or all of it into microbial biomass. ~~The p~~Peptide-like ~~microbially-produced~~ formulas comprised 22 – 40 % of the bio-produced formulas (Table S2 in the Supplement). ~~, and t~~The results of the comparative analyses described above ~~also~~ imply that these proteinaceous formulas are of highly variable composition. Their molecular diversity is additionally evaluated using one-way analysis of variance (ANOVA) reported in Sect. 6 of the Supplement. This statistical ~~tool-analysis indicated~~ revealed high molecular variability supporting the findings by the presence-/absence comparisons presented earlier (Table 1). ~~The results from these statistical assessments support the findings by the presence/absence comparisons and-Collectively,~~ these findings ~~collectively~~ conclude that the microbial incubations of pyDOM created pools of new, very diverse molecules, a process hereafter referred to as “microbial diversification”. As

414 FT-ICR-MS was performed with soft electrospray ionization with no fragmentation, the structure of the observed  
415 molecules is inferred from the elemental composition of the assigned molecular formulas. Another possibility for  
416 these N-containing molecules is that they were formed by ~~radical processes that coupled~~ coupling reactions among  
417 pyDOM molecules with the  $\text{NH}_4^+$  nutrient that was added to support microbial growth (e.g., via Michael addition  
418 reactions; McKee et al., 2014). ~~A preliminary experiment (data not shown) showed that mixing pyDOM with~~  
419  ~~$\text{NH}_4^+$  did not result in abiotic formation of new molecules (for example via Michael addition; McKee et al., 2014),~~  
420 ~~but abiotic formation was not tested in the presence of radicals.~~

421 To confirm that these bio-produced formulas were associated with proteinaceous structures and are not  
422 just N-containing compounds that coincidentally plotted in the <sup>2</sup>peptide region<sup>2</sup>, spectrofluorometric analysis was  
423 performed to obtain excitation-emission matrices (EEMs) of the pyDOM samples before and after bio-incubation  
424 (Fig. 2). The data for Oak 650 Photo is not reported as the produced EEM spectra were of questionable quality,  
425 and as the sample was in very limited amounts, analytical ~~validation~~ replication and quality assessment were not  
426 possible.  
427



428



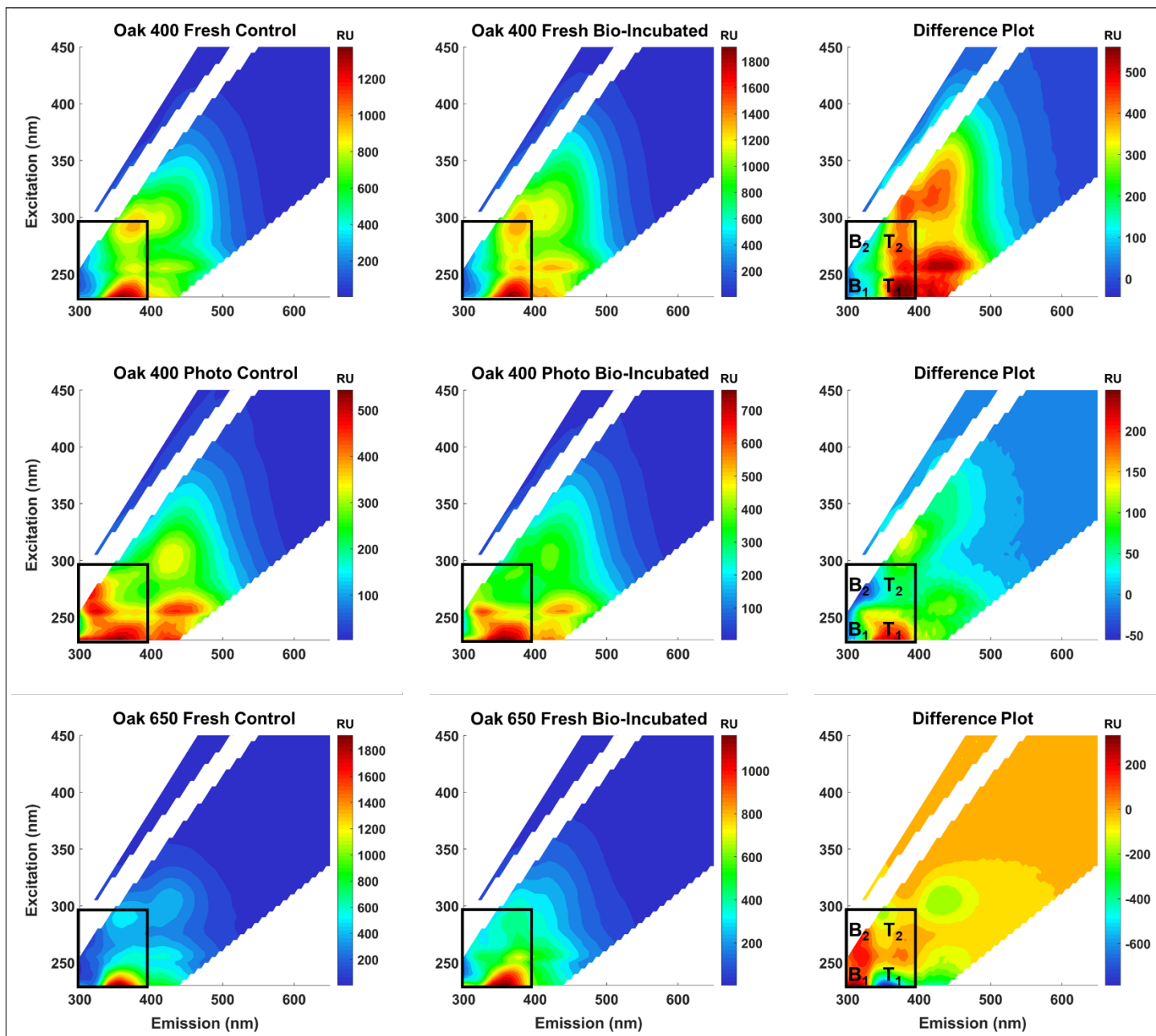


**Figure 2.** Fluorescence excitation-emission matrices (EEMs) of control (left panels) and bio-incubated (middle panels) pyDOM samples. Difference spectra are shown in the right panels. The black box indicates the region where compounds of proteinaceous ~~and autochthonous/microbial~~ origin fluoresce (Coble, 1996; Coble et al., 2014), with tyrosine-like (B<sub>1</sub> and B<sub>2</sub>) and tryptophan-like (T<sub>1</sub> and T<sub>2</sub>) peaks labeled on the difference plots (~~right panels~~).

Proteinaceous organic matter has a highly characteristic fluorophoric signature due to the distinguishable signals of the aromatic amino acids tyrosine and tryptophan. The short Stokes' shifts of these fluorophores allow them to spectroscopically separate on the EEM plot allowing for identification of related labile substances (Wünsch et al., 2019). Other amino acids, namely histidine and phenylalanine, are also fluorophoric, but are not easily identified in EEM data of complex matrices. A simplistic-practical approach to evaluate the change after the bio-incubation is to use difference plots (e.g., Hemmler et al., 2019). For all samples, strong proteinaceous signals evolve after biotic incubations indicating that molecules of of proteinaceous and autochthonous (~~microbial~~) origin are produced (Coble, 1996; Coble et al., 2014). This indicated that peptide-like molecules observed using FT-ICR-MS are not an-artifact artificially produced by coupling reactions growth (e.g., via Michael

445 addition reactions; McKee et al., 2014) or evolve due to less-~~due to~~ charge competition in the ESI source. Thus,  
446 the protein-like formulas, ~~but~~ are truly bio-produced, validating the findings of the presence/~~absence~~ analysis.

447 There are subtle differences among the EEMs of all control and bio-incubated samples indicative of the  
448 high variability in fluorophoric content of these samples. This agrees with the observed variability in molecular  
449 composition described earlier. An interesting observation is that in the two Oak 400 pyDOM incubations,  
450 tyrosine-like fluorescence (peaks B<sub>1</sub> and B<sub>2</sub>) decreases after biotic incubation while-whereas tryptophan-like  
451 fluorescence (peaks T<sub>1</sub> and T<sub>2</sub>) increases. In contrast, the tryptophan-like fluorophores are degraded and tyrosine-  
452 like ones are produced after biotic incubation of Oak 650 Fresh pyDOM. It must be noted that there are  
453 proteinaceous fluorophores (and peptide-like formulas) in the control samples resulting from the addition of the  
454 microbial inoculate, but the associated fluorophores were present in low amounts. Thus, proteinaceous  
455 fluorescence signals in the control samples are not unexpected. However, a decrease in proteinaceous  
456 fluorophores is opposite of what is expected after significant microbial growth. Proteinaceous compounds are  
457 highly bio-labile and aromatic compounds are susceptible to oxidation by ROS. Therefore, it is possibly-possible  
458 that tyrosine-like fluorophores (in Oak 400 pyDOM) and tryptophan-like fluorophores (in Oak 650 pyDOM) are  
459 still actively participating in bio-degradation processes as the incubations were still active at the time of sampling  
460 (10 days). ~~due to fluorophoric compounds in this system being highly bio-labile and/or susceptible to oxidation~~  
461 by specific ROS, but the residual post-oxidation by products would be still detectable by FT-ICR-MS and  
462 classified as peptide-like compounds. The loss of tyrosine-like fluorophores in the Oak 400 samples, and loss of  
463 tryptophan-like fluorophores in the Oak 650 Fresh sample, are indicative of different microbial physiology and  
464 exudates ~~in these incubations~~. The complexity of these EEM spectra and the compound-specific changes observed  
465 here indicate that proteomic and/or metabolomic analyses (e.g., Nalven et al., 2020) are necessary in future  
466 microbiological studies ~~of pyDOM~~ in order to fully understand the changes ~~in to the~~ molecular composition of  
467 pyDOM during such biotic incubations.

468 To determine if the bio-produced formulas are from true proteins, or are from compounds with residual  
469 proteinaceous fluorophores, the formulas were evaluated in the context of possible combinations of amino acids  
470 that would be singly charged. Given that microbes exude large proteins (molecular weightMW > 30 kDa) such  
471 as lignin peroxidases, manganese peroxidases, and laccases (Higuchi, 2004), the peptide-like formulas observed  
472 by FT-ICR-MS (analytical window of 200-1000 Da) may have resulted from hydrolysis of the above-mentioned  
473 enzymes (or other proteinaceous exudates). If that is the case, the hydrolysates would likely have had a simple  
474 oligomeric composition. To test this, the bio-produced peptide-like formulas in each sample were compared to a  
475 library of 888,009 possible combinations of 20 amino acids (oligomeric sequences of 2-7 residues). Only a small  
476 number of oligopeptides were identified (5 – 18 oligopeptides of 2 – 5 amino acids, Tables S2 and S3 in the  
477 Supplement) which is counter to the proposed idea that hydrolysis of microbial exudates produced these newly  
478 observed peptide-like formulas. Therefore, the observed bio-produced formulas may represent compounds with  
479 residual proteinaceous fluorophores and are not true oligopeptides. The lack of identified oligopeptides also calls  
480 into question the idea that microbial processes were solely responsible for the high variability of the bio-produced  
481 organic matter observed after the microbial incubation of pyDOM.

482 In an attempt to To further elucidate the composition of these bio-produced N-containing substances, we  
483 re-evaluated the previously published <sup>1</sup>H NMR data of these samples (Bostick et al., 2020a2021) in greater detail.  
484 Additionally, ~~to further elucidate~~ the connectivity between previously observed functional groups, was assessed  
485 using two-dimensional <sup>1</sup>H-<sup>1</sup>H total correlation NMR spectroscopy (TOCSY) ~~was utilized~~ on a select sample.  
486 Figure 3 shows the TOCSY spectra of the bio-incubated Oak 650 Fresh sample.

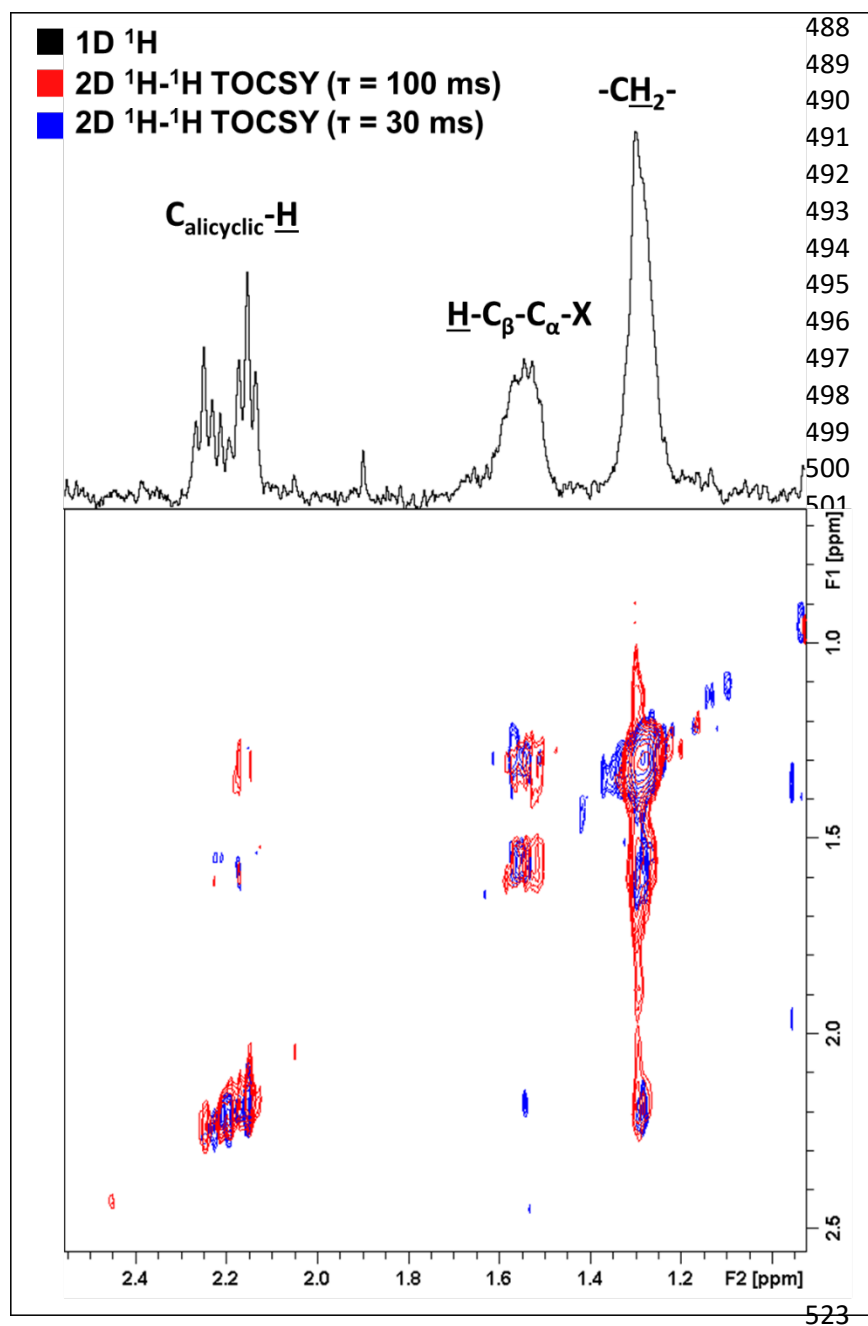


**Figure 3.** Two-dimensional  $^1\text{H}$ - $^1\text{H}$  total correlation spectroscopy (TOCSY) NMR spectra of the bio-incubated Oak 650 Fresh sample. Short- and long-range couplings were allowed to evolve during mixing times ( $\tau$ ) of 30 (blue) and 100 ms (red), respectively. The 1D  $^1\text{H}$  spectrum is shown as a projection on top (black).

There are three groups of resonances representing an alicyclic structure, a  $\beta$ -hydrogen to a heteroatom, and a methylene group that were found in all samples, even in the controls (although of small contributions relative to the total spectral signal). These resonances have not been previously observed in the  $^1\text{H}$  NMR spectra of these pyDOM samples (Bostick et al., 2018; Goranov et al., 2020) indicating that they represent by-products of the microbial incubations, likely microbial biomass. In the control samples, the compounds associated with these resonances must be from the soil inoculant that was added. The three resonances are also observed to be in the same coupling network indicating that they are a part of the same or similar structures. Due to the very low concentration of these samples ( $3.5 - 4 \text{ mgC}\cdot\text{L}^{-1}$ ), the NMR analysis did not allow for a high-resolution structural elucidation, but some distinct signatures were nonetheless observed. The deshielded aliphatic peaks at  $\delta = 2.1 - 2.3 \text{ ppm}$  have a complex multiplicity pattern, a characteristic feature of alicyclic structures. These are likely residual carbohydrate moieties which have lost most of their O-containing groups through various cleavage processes and their backbone  $\text{C}_{\text{alicyclic}}\text{-H}$  resonances have been shifted upfield. The peak at 1.55 ppm is from  $\beta\text{-H}$  hydrogens to a heteroatom ( $\text{H-C}_{\beta}\text{-C}_{\alpha}\text{-X}$ , where  $\text{X} = \text{O}, \text{N}, \text{S}$ ), and these are known to be associated with

538 peptidoglycans (Spence et al., 2011). The TOCSY analysis was performed with two different mixing times ( $\tau =$   
539 30 and  $\tau = 100$  ms) in order to evaluate short-range (2 – 3 bond) and long-range (4 – 6 bond) connectivities. Based  
540 on the observed couplings the observed resonances are vicinal to each other (3 bonds away). This indicates that  
541 these functional groups are closely bound in the peptidoglycan substances they likely represent.

542 All of these ~~analyses-assessments described above of the molecules observed after the biotic incubation~~  
543 ~~of the four pyDOM samples~~ conclude that the observed biochemical processes in these pyDOM systems  
544 incubations are complex and difficult to unambiguously interpret. Based on ~~our~~ findings, ~~above it is clear that~~  
545 ~~we summarize that~~ these bio-produced formulas (Figure 1) can originate from three different possible sources:

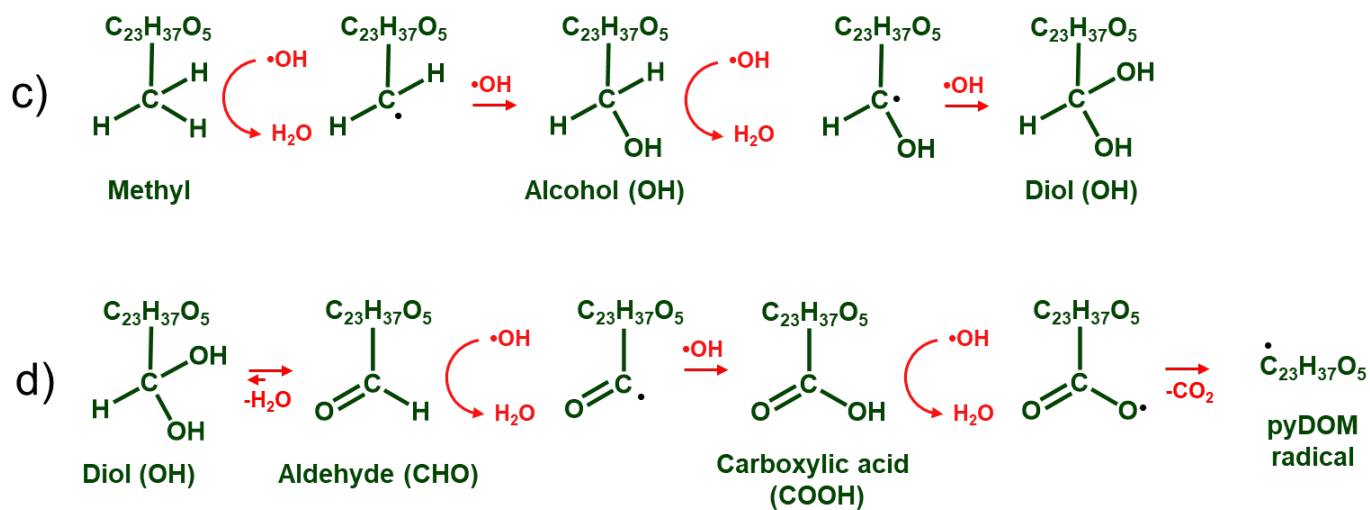
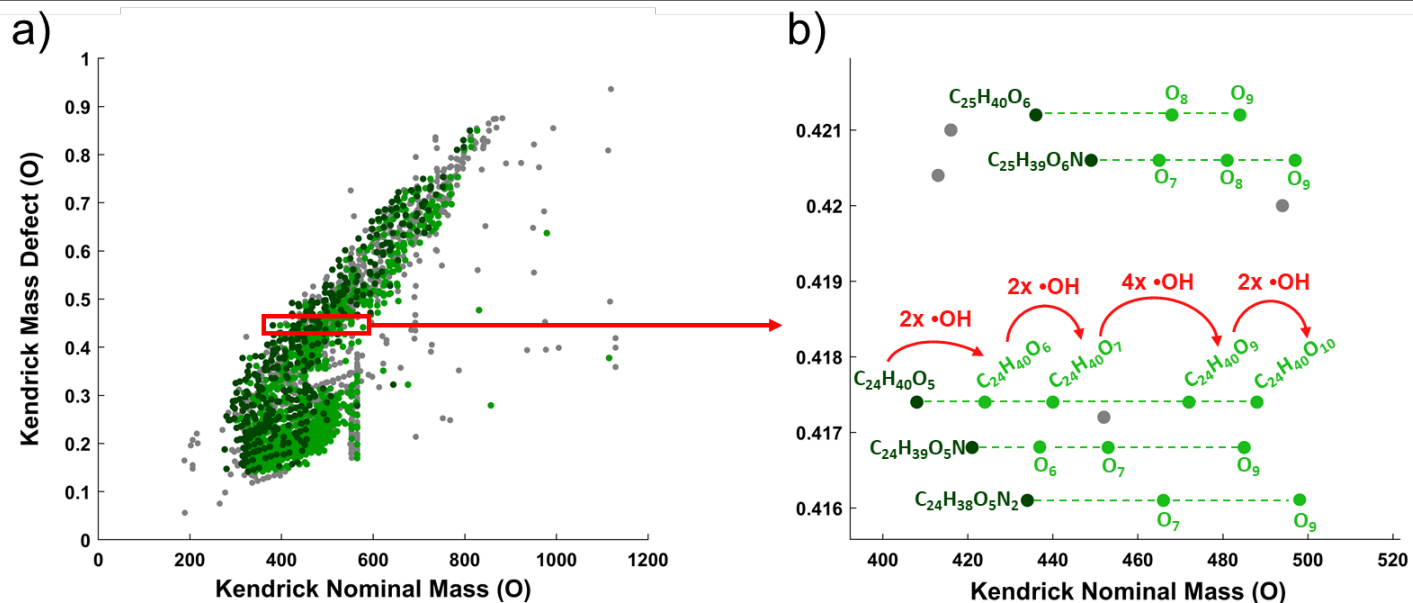
- 546 1) exoenzymes, which microbes use to extracellularly degrade larger molecules into smaller ones (Hyde and  
547 Wood, 1997; Higuchi, 2004);
- 548 2) peptidoglycans, which likely leached into solution after bacterial death and cell lysis (Yavitt and Fahey,  
549 1984); and
- 550 3) other metabolites and exudates involved in the physiology of the different microbes in the used consortium  
551 (e.g., signaling compounds).

552 The significant degradation of pyDOM and production of these biological compounds indicates that microbes  
553 successfully converted the presumably carbon-rich recalcitrant pyrogenic molecules into more labile substances,  
554 a process we define as hereafter refer to as “microbial labilization”. However, the fact that the observed bio-  
555 produced labile molecules are not identifiable as simple oligopeptides, and are present in significantly different  
556 composition among the four samples, suggests that this molecular diversity may not be caused by predictable  
557 biotic reactions but by random radical-driven processes. Further evidence for the random radical-driven processes  
558 comes from the observed degradation of molecules across the whole vK space (Figs. 1 and S2), which is unusual  
559 because microbes generally preferentially consume smaller aliphatic species (Berggren et al., 2010a,b; Kirchman,  
560 2018).

### 561 3.3 Radical oxygenation as a potential source of molecular diversity

562 Microbial physiology has been associated with the production of reactive oxygen species (ROS), which  
563 have been shown to be important in the degradation of various types of organic compounds (e.g., Scully et al.,  
564 2003; McNally et al., 2005; Porcal et al., 2013; Trusiak et al., 2018; Xiao et al., 2020). ~~A recent~~ study-studies  
565 showed that radicals can degrade various types of ligninaceous molecules (Waggoner et al., 2015, 2017;  
566 Waggoner and Hatcher, 2017~~Waggoner et al., 2017~~) suggesting that microbially induced radical reactions can  
567 target a variety of pyDOM molecules as well. While there were no ROS measurements made in this study, we  
568 have performed Kendrick Mass-mass Defect-defect (KMD) analysis of the FT-ICR-MS data (Kendrick, 1963;  
569 Hughey et al., 2001) to seek evidence for radical action processes. The KMD analysis identifies formulas that  
570 differ by any repeating structural moiety (e.g.,  $-\text{CH}_2-$ ). To identify potential products of radical attacks, we have  
571 evaluated the FT-ICR-MS data in the context of oxygenation, i.e., searched the mass lists for formulas differing  
572 by one oxygen atom (addition of hydroxyl group), carbonyl group (addition of aldehydes or ketones), and  
573 carboxyl groups (Fig. 4).  
574  
575  
576





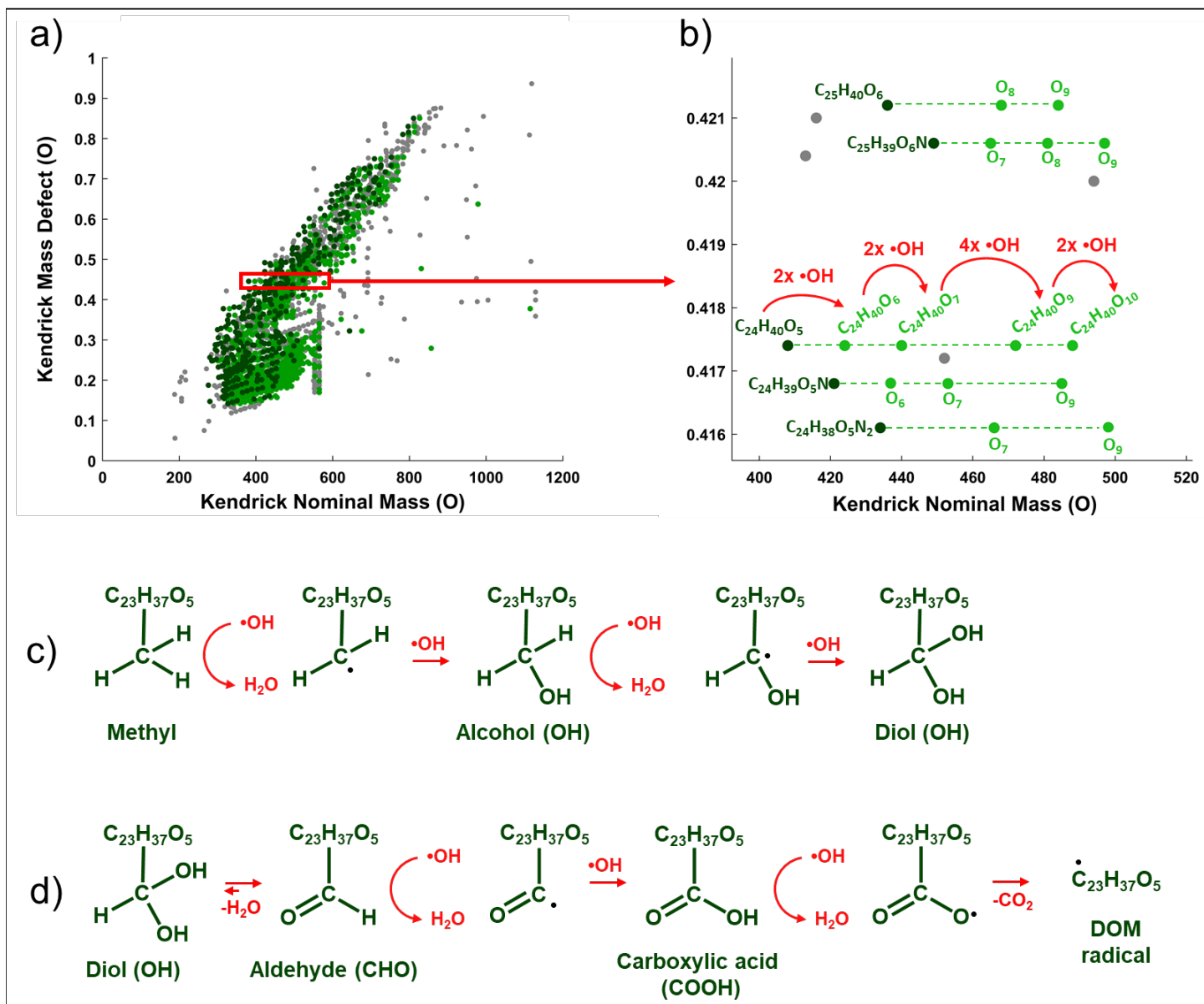
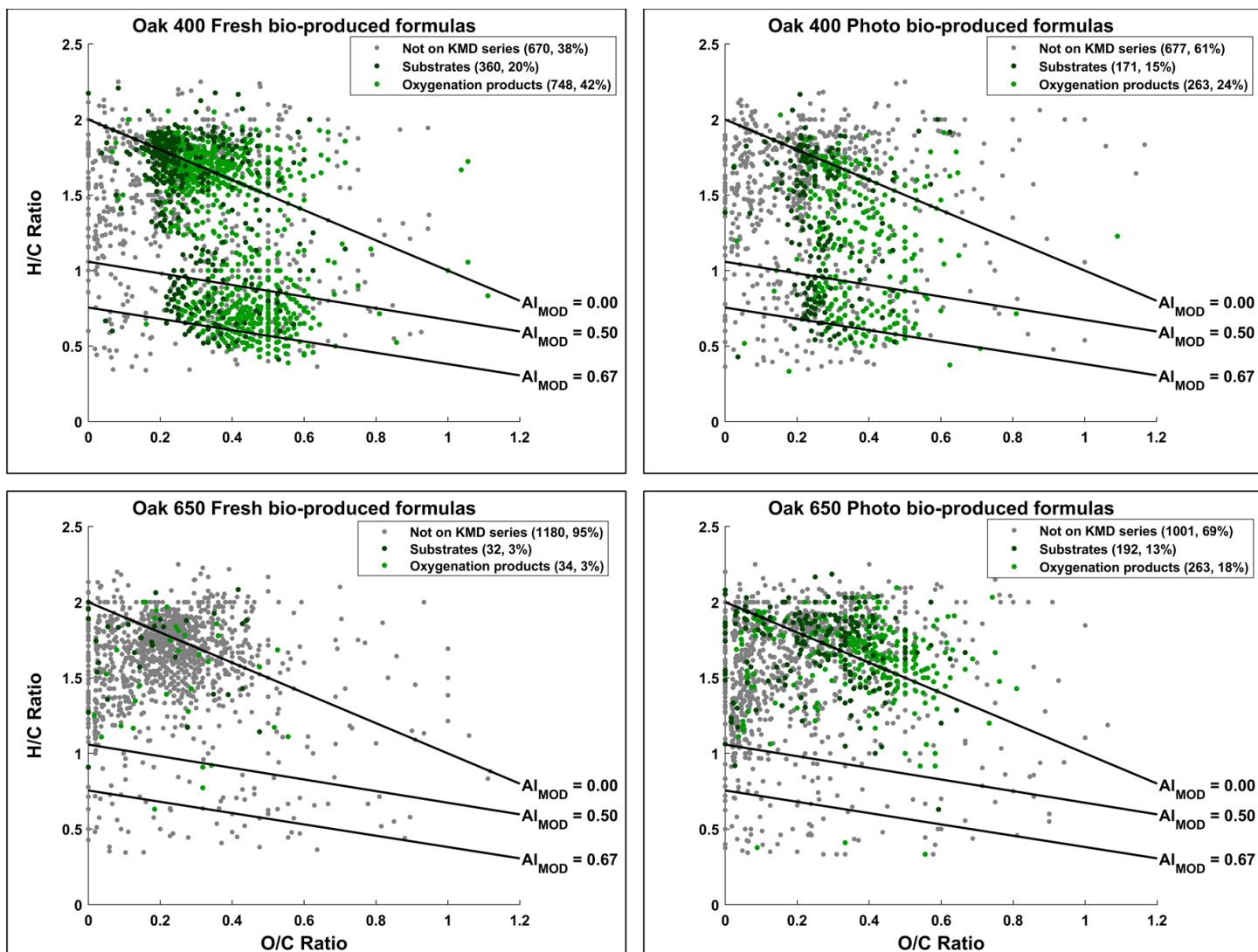


**Figure 4.** Kendrick ~~Mass-mass Defect-defect~~ (KMD) analysis using oxygen (O) series of the bio-produced formulas of Oak 400 Fresh pyDOM. Panel a) shows the whole KMD plot while panel b) shows an expanded region of it. Formulas not part of the O KMD series are colored in **gray**. Formulas in **dark green** are proposed substrates, and their oxygenation products are colored in **light green**. Only the molecular formulas for one of the series (KMD = 0.4174 Da) are labeled ~~on panel b)~~, while for the rest of the molecules, only the substrate formula and the number of oxygens in the oxygenation products are listed for clarity. The red arrows ~~in panel b)~~ show the formation of the four oxygenation products of the  $C_{24}H_{40}O_5$  substrate after a sequential attack by hydroxyl radicals ( $\cdot OH$ ). Panel c) shows possible chemical reactions that can cause an increase of number of oxygens. Panel d) shows further oxidative processes involving the formation of keto and carboxyl groups ~~which can contribute to the degradation of pyDOM, as well which processes ultimately produce pyDOM radicals and  $CO_2$  as to the formation of DOM.~~ The KMD plots for all samples are shown on Figs. S10-12 in the Supplement.

The mathematics behind the KMD analysis (see Sect. 2.4) convert the mass of the molecular formula (also known as the IUPAC mass) to a “Kendrick” mass placing the formula on a scale that is, whose which mass is on a different scale which is specific for the selected structural moiety. On Fig. 4a, an example is shown with the KMD analysis for molecules differing by one oxygen (-O-). On the regular (IUPAC) mass scale, such formulas would differ by 15.994915 Da, but on the Kendrick “O” mass scale, they differ by 16 Da. The difference between

596 the Kendrick ~~Massmass, KM~~ (e.g., ~~KM = 408.2876 Da~~) and the Kendrick ~~Nominal-nominal Massmass, KNM~~  
597 (e.g., ~~KNM = 408 Da~~) is the Kendrick ~~Mass-mass Defectdefect~~, KMD (i.e., ~~KMD = 0.2876 Da~~), ~~and f~~Formulas  
598 with the exact same KMD differ by one or more oxygens, and lie on a KMD series. Visually these formulas would  
599 plot on horizontal lines on the KMD plot as indicated by the dashed lines in Fig. 4b. Taking the series of KMD =  
600 0.4174 ~~Da as an example~~, ~~this~~ ~~KMD~~ evaluation shows that there are five formulas in this particular KMD series  
601 that differ in number of oxygens ( $C_{24}H_{40}O_{5-10}$ ). This implies that once  $C_{25}H_{40}O_5$  is produced, it acts as a substrate  
602 and the other four formulas ( $C_{24}H_{40}O_{6-10}$ ) are produced by oxygenation (likely in a sequential manner:  $C_{24}H_{40}O_5$   
603  $\rightarrow C_{24}H_{40}O_6 \rightarrow C_{24}H_{40}O_7 \rightarrow C_{24}H_{40}O_9 \rightarrow C_{24}H_{40}O_{10}$ ). ~~Such formulas differing in the number of oxygens can be~~  
604 ~~formed This can happen~~ via oxygenation by hydroxyl radical ( $\bullet OH$ ) attacks (~~Waggoner et al., 2015, 2017;~~  
605 ~~Waggoner and Hatcher, 2017~~). This ROS can abstract a hydrogen from C-H bonds and the hydrogen is substituted  
606 with an OH-group, resulting in the formation of alcohols (C-OH) as shown in Fig. 4c. This is ~~likely the suggested~~  
607 ~~pathway of~~ how the oxygenation products shown in Fig. 4a and 4b have formed. Evidence for such reactions will  
608 be found on the KMD plots as evolution of ~~a new molecules~~ within the same KMD series, but with a different  
609 number of oxygens. Further radical attacks ~~would produce results in formation of~~ polyols (Fig. 4c). In the case of  
610 formation of geminal diols (two alcohol groups on the same carbon atom), they can rearrange to aldehydes or  
611 ketones via keto-enol tautomerism (Fig. 4d). Further radical attacks would produce carboxyl groups, which can  
612 also be radically cleaved, and ~~py~~DOM radicals be formed. ~~Py~~These-DOM radicals (as well as any other radical  
613 intermediate in this pathway) can be then further paired with hydrogen radicals ( $\bullet H$ ) from the solution, other  $\bullet OH$   
614 radicals, or other radicalized pyDOM or proteinaceous species.

615 Using KMD analysis, formulas ~~produced that could have been produced~~ by oxygenation were identified  
616 and plotted individually (Fig. 5). It is assumed that the smallest molecule in each series is the substrate and any  
617 molecules with ~~more increasing number of~~ oxygens are oxygenation products.  
618



619  
620 **Figure 5.** Van Krevelen diagrams ~~evaluating~~ ~~showing~~ oxygenation products among the bio-produced formulas  
621 of the four incubated pyDOM samples. Formulas not part of any of the oxygenation KMD series (O, CO, or COO)  
622 are colored in **gray**. Formulas in **dark green** are substrates with their oxygenation products colored in **light green**.  
623 The number of formulas in each of these pools are shown in the legends (along with corresponding percentages).  
624 The black lines indicate modified aromaticity index cutoffs ( $AI_{MOD}$ ; Koch and Dittmar, 2006, 2016).  
625

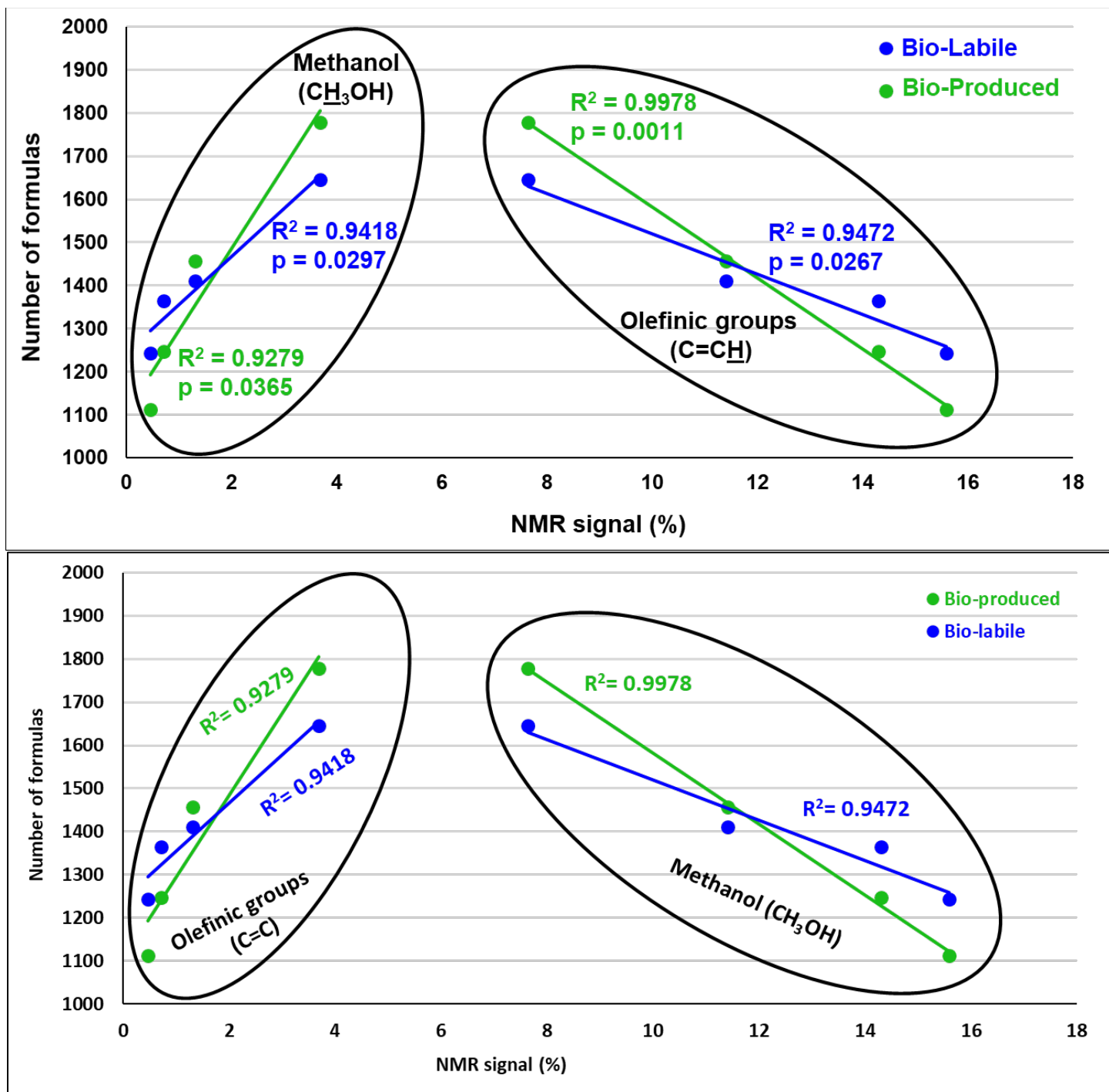
626 KMD analysis revealed that about a third (34 – 748, 3 – 42%) of the bio-produced formulas ~~in these~~  
627 ~~pyDOM samples~~ could be classified as products of oxygenation reactions, likely driven by ROS species such as  
628 the hydroxyl radical ( $\bullet OH$ ). This is in agreement with previously observed cross-linking of microbial compounds  
629 through oxidative processes (Sun et al., 2017). The majority of the ~~bio-produced~~ formulas, however, were not  
630 found to be products of oxidation as they did not lie on ~~neither any~~ of the evaluated KMD series (O, CO, ~~nor~~  
631 COO). Therefore, the ~~majority of the bio-produced se-compounds formulas~~ are likely formulas of exudates which  
632 were resistant to radical attacks or are formulas of compounds which have already been radically coupled with  
633 other compounds to result in unrecognizable molecules by the KMD analysis.

634 Additional evidence for intense radical processes in these systems is the evolution of bio-produced  
635 unsaturated aliphatic compounds ( $1 < H/C < 2$ ,  $O/C < 2$ ) on the vK diagrams (Figs. 1 and S4). ROS can attack  
636 aliphatic and aromatic compounds, open aromatic and alicyclic rings, cleave oxygen- or nitrogen-containing  
637 functionalities, and produce highly aliphatic molecules, as previously observed after photo-irradiation of pyDOM  
638 (Goranov et al., 2020), ConAC (Zeng et al., 2000a,b), and radical-based degradation ~~studies~~ of lignin (Waggoner  
639 et al., 2015, 2017; Waggoner and Hatcher, 2017; Khatami et al., 2019a, b). ROS can also attack any of the



640 proteinaceous exudates and peptidoglycans cleaving them from many of their functional groups and converting  
641 them into the observed unsaturated aliphatic compounds. These produced aliphatic compounds could also  
642 contribute to the newly produced N-containing (“peptide-like”) compounds observed by FT-ICR-MS if they are  
643 oxygenated by ROS post-formation. However, this seems unlikely as data from the supplementary fluorescence  
644 and NMR analyses support the formation of microbial biomass. The KMD analysis shown here strongly suggests  
645 the presence of ~~se indirect observations of~~ intense radical processes as formulas with increasing numbers of  
646 oxygen atoms are known to be formed following radical oxygenation (Waggoner et al., 2015, 2017; Waggoner  
647 and Hatcher, 2017).~~indicate that the microbial incubations of pyDOM are extremely complex systems~~ However,  
648 it must be noted that this KMD analysis does not directly prove the existence of radical processes and the  
649 suggested radical processes are speculated based only on indirect observations. Future studies need to directly  
650 test the presence of radical reactions by performing biotic incubations of pyDOM with radical quenchers as well  
651 as by quantifying radical fluxes in these microbiological systems., and future studies need to employ specialized  
652 more bio-analytical techniques to fully understand the processes occurring in them.

653 While FT-ICR-MS peak magnitudes are considered to be semi-quantitative a function of molecular  
654 ionizability, making it generally impossible to quantify the different bio-labile and bio-produced compounds of  
655 our study, the ultrasensitivity of this technique ensures detection of all compounds that are within its the FT-ICR-  
656 MS analytical window. Here, the number of molecular formulas can be used as a quantitative measure for  
657 molecular diversity (e.g., Gurganus et al., 2015). Previously published liquid-state <sup>1</sup>H NMR data for the same  
658 samples (Bostick et al., 2020a2021) provide a quantitative measure of functional group content. SignificantStrong  
659 positive and negative correlations were observed between the numbers of bio-labile and bio-produced formulas  
660 and the percent NMR spectral signal accounted for by olefinic functionalities and methanol, respectively (Fig. 6  
661 and Table S4). These correlations suggest that the diversity of bio-degraded (bio-labile) and bio-produced  
662 molecules was related in some way with a process related to the availability of methanol (CH<sub>3</sub>OH) and olefinic  
663 functionalities (C=C) in pyDOM.



665  
666  
667  
668  
669  
670  
671  
672  
**Figure 6.** Pearson correlation analysis between the number of **bio-labile** and **bio-produced** formulas detected by FT-ICR-MS and relative intensity (in %) of olefinic functionalities (C=C) and methanol (CH<sub>3</sub>OH) as measured by liquid-state <sup>1</sup>H NMR and reported by Bostick et al. (2020a,2021). No significant correlations were found between other functional groups and the number of bio-produced or bio-labile formulas (data shown in Table S4 of the Supplement).

673  
674  
675  
676  
677  
Olefinic functionalities have been recently identified as important structural motifs in the composition of pyDOM and were observed to degrade in photochemical experiments likely due to their high reactivity with ROS species (Goranov et al., 2020). Although they-olefins are in low abundance in pyDOM (< 10%), it is likely that they act as important intermediates in the degradative pathways of pyDOM. The olefinic bonds can be homolytically cleaved when attacked by radicals and effectively act as radical-accelerators that further propagate

678 radical-mediated organic matter transformations. Thus, the abundance of olefins can further increase the  
679 abundance of radicals and contribute to the elevated molecular diversity resulting in the ~~linear~~  
680 ~~relationships~~significant correlation shown in Fig. 6.

681 The other significant correlation between molecular diversity and NMR data is observed to be with  
682 methanol (CH<sub>3</sub>OH), a very sharp highly distinguishable singlet at  $\delta = 3.34$  ppm in <sup>1</sup>H NMR spectra (Gottlieb et  
683 al., 1997). As it is a common contaminant in NMR analysis, special precautions were taken to obtain ultraclean  
684 spectra (see Sect. 2.5). Methanol is a species that is naturally present in pyDOM (Bostick et al., 2018), and while  
685 it is generally considered to be toxic to microbes (Dyrda et al., 2019), there are methylotrophic bacteria and fungi  
686 (microbes of the families *methylococcaceae* and *methylobacteriaceae*) that can utilize it as a substrate  
687 (Chistoserdova et al., 2003; Kolb and Stacheter, 2013; Chistoserdova and Kalyuzhnaya, 2018). These species  
688 have been previously observed in the soil from the area where the microbial inoculum was extracted from  
689 (Khodadad et al., 2011); suggesting that the degradation of methanol may be biotic. In fact, in these samples,  
690 methanol, along with the other two measured ~~low-molecular-weight~~LMW substances, acetate and formate, was  
691 nearly-almost completely degraded over the 10-day incubation (Bostick et al., ~~2020a~~2021).

692 The inverse relationship between the content of methanol and molecular diversity (Fig. 6) can be  
693 interpreted in several ways. Firstly, methanol could be exhibiting toxicity to the microbes that assimilate pyDOM,  
694 as has been observed previously (Dyrda et al., 2019). This, however, is unlikely for the pyDOM systems studied  
695 here because the sample with the highest amount of methanol (Oak 400 Photo, ~3.7% CH<sub>3</sub>OH) was the second  
696 most bio-reactive (Bostick et al., ~~2020a~~2021). Instead, the observed strong-significant negative correlation may  
697 be explained by the fact that methanol is a known radical-scavenger (Múčka et al., 2013). If, as we propose, the  
698 molecular diversity results from the activity of radical processes, an increasing concentration of methanol would  
699 quench ~~these radicals~~ROS thereby decreasing ~~their-the radical~~ activity and limiting the molecular diversity in  
700 these systems. ~~This would explain the negative relationship depicted by the correlation shown in Fig. 6.~~

## 701 4 Discussion

### 702 4.1 Multiple pathways for the alteration of pyDOM by microbes

703  
704 Using a variety of analytical platforms in this and the parallel study (Bostick et al., ~~2020a~~2021), significant  
705 quantitative and qualitative losses were observed when pyDOM was subjected to incubation with a microbial  
706 consortium collected from a site impacted by ~~forest-fires~~wildfires. Additionally, labile and diverse compounds  
707 were produced during these incubations. Due to the high complexity of pyDOM, the changes are not  
708 straightforward, and there are at least two important-degradation pathways at play: 1) degradation through  
709 microbial assimilation (consumption of pyDOM), and 2) degradation/transformation via radical-mediated  
710 reactions (e.g., oxygenation) by ROS produced from microbial exoenzymes. These two pathways are discussed  
711 in the context of degradation of pyDOM and formation of new labile and diverse molecules.

#### 712 4.1.1 Molecular degradation of pyDOM

713  
714 A surprising observation in this study is that there was a uniform loss of pyDOM molecules from all  
715 regions of the vK diagrams. Microbes, it is generally presumed, preferentially assimilate small non-aromatic  
716 substances such as carbohydrates, proteins, and low-molecular-weightLMW acids (Berggren et al., 2010a,b;  
717 Kirchman, 2018). Thus, the aromatic fraction of pyDOM, mainly the ConAC, are generally considered to be bio-  
718 ~~recalcitrant-resistant~~ (Goldberg, 1985; Masiello, 2004). In addition to the condensed character of many of the  
719 molecules, there are significant numbers of potentially toxic organochlorine compounds, of both aliphatic and  
720 aromatic character, in pyDOM (Wozniak et al., 2020). Thus, the finding of the major biological activity in these  
721 pyDOM samples systems and the significant amount of carbon, including aromatic carbon, that was mineralized,  
722 is a very significant finding for the wildfire biogeochemistry community (Bostick et al., ~~2020a~~2021).

723 Although pyDOM is highly heterogeneous (Wozniak et al., 2020), the observation of diverse molecular  
724 consumption-bio-degradation is not unique to it. In a recent microbial degradation study of snow DOM, Antony

et al. (2017) observed that both aromatic (including ConAC, lignin, and tannins) and aliphatic formulas were biodegraded. This is likely due to microbes evolving chemical mechanisms to thrive under in the extreme glacial conditions of glaciers (Antony et al., 2016). Analogously, as there have been previous prescribed fires in the area from which the microbes for this study were extracted (Johns, 2016), it is also possible that our organisms microbes have had adapted to the presence of ConAC and other pyrogenic substances pyOM, by developing mechanisms for their assimilating the carbon in large, complex molecules including ConAC on (Judd et al., 2007).

While direct microbial assimilation of pyDOM compounds is certainly likely to have occurred, our molecular and spectroscopic data show findings suggest that there was likely a second degradative pathway which likely contributed contributing to the extensive molecular alteration, and to the significant loss of carbon that was quantified in the parallel study (Bostick et al., 2020a2021). While some microbial exoenzymes operate via hydrolytic pathways (amylases, lipases, proteases, cellulases,  $\beta$ -galactosidases, etc.), many other enzymes operate through oxidative (electron-withdrawing) pathways. Examples of such enzymes are the various lignin-modifying enzymes in the peroxidase (lignin peroxidases, manganese peroxidases, etc.) and phenoloxidase (e.g., laccases) families (Higuchi, 2004). Thus, reactive oxygen species ROS are usually produced and involved in the microbial degradation of organic matter in the environment.

The bio-labile molecules in the studied pyDOM samples are of highly variable degrees of oxygenation, aromaticity, and size. There were large MW compounds (~~some~~ MW > 550 Da) that were degraded indicating that ~~Thus~~, microbial exoenzymes producing ROS would have been needed to reduce the size of these large substrates into smaller units that could pass through microbial cell membranes and be consumed by the biota (Sinsabaugh et al., 1997; Fuchs et al., 2011; Burns et al., 2013) ~~and be consumed by the biota~~. The presence of enzymatic compounds is confirmed by observation of peptide-like compounds (FT-ICR-MS analysis) and proteinaceous fluorophores (spectrofluorometric analysis). An important finding is that a preferential degradation of ConAC of smaller molecular weights MW was observed (Bostick et al., 2020a2021). As small ConAC (i.e., oxygenated PAHs polycondensed aromatic hydrocarbons) are known to be toxic (e.g., Idowu et al., 2019), it is unlikely that they were directly consumed by the microbes. Oxygenated polycondensed aromatic hydrocarbons These substances are highly susceptible to attacks by ROS, which is likely how they were degraded in these samples. Thus, we speculate that microbes are most likely not directly consuming the smaller ConAC, but rather, are smaller ConAC are degrading them degraded indirectly using via ROS oxidation. Furthermore, ROS These radicals can oxygenate pyDOM with various functional groups (e.g., hydroxy, aldehyde/keto, carboxyl), and can also cleave functional groups (e.g., methoxy functionalities), open aromatic rings, and completely mineralize compounds to inorganic carbon (CO, CO<sub>2</sub>, HCO<sub>3</sub><sup>-</sup> and CO<sub>3</sub><sup>2-</sup>) as shown on Fig. 4. ROS have been previously shown to be very important in pyDOM photochemistry (Ward et al., 2014; Fu et al., 2016; Goranov et al., 2020; Wang et al., 2020), and it is likely we speculate that they play an important role in the microbial degradation of pyDOM as well.

More indirect evidence for radical species involvement is provided by the peptidoglycan molecules produced during the pyDOM incubations. While these Peptidoglycan molecules are generally large (Vollmer et al., 2008) and would not be detected as singly-charged molecules ions using FT-ICR-MS (analytical window covering only m/z 200-1000), ~~their~~ hydrolytic products of peptidoglycans though (small oligopeptides) would be observed. Very few peptide sequences (5 – 18 oligopeptides of 2 – 5 residues) were identified among the bio-produced formulas indicating that such hydrolysates did not exist in the samples at the time of measurement. However, if there were abundant radical reactions occurring in the system, as we suggest, it is very possible that these hydrolysates were altered into unrecognizable organic structures that would still be classified as “peptide-like” but would have different molecular composition than the predicted linear peptide sequences. It is also possible that instead of peptidoglycan hydrolysis followed by consecutive oxygenation, ROS directly cleaved the peptidoglycans into smaller non-linear substances of peptide-like molecular composition.

It must be noted that the results of our study were acquired using negative-mode ESI which is only effective for electronegative (carboxyl-rich, hydroxyl-rich) compounds (Stenson et al., 2002; Patriarca et al., 2020). Thus, the trends of degradation and labilization are skewed to fit this criterion and do not provide a complete overview of all molecules that are bio-labile or bio-produced. Future studies should employ positive-



mode ESI and/or different ionization sources (such as atmospheric pressure photoionization) to better elucidate the molecular degradability of pyDOM.

#### 4.1.2 Labilization and Diversification of pyDOM

The production of labile unrecognizable biological substances during these incubations correlates well with previous findings showing the formation of thousands of new biological compounds during biotic incubations unrelated to microbial metabolic pathways (Lechtenfeld et al., 2015; Wienhausen et al., 2017; Patriarca et al., 2021). ~~However, in difference with previous studies, it was found that an~~ ~~There was no~~ insignificant overlap ~~amongof the~~ bio-produced formulas ~~was observed amongof~~ the four pyDOM samples ~~after the incubations~~ (2 – 320 formulas in common, 0 – 12%). Insignificant numbers of ~~matching bio-produced~~ formulas from pyDOM were also found in the bio-produced formulas of an incubation of sucrose with the same soil microbes (63 – 94 formulas, 3%). This indicates that microbes diversified the composition of ~~these the~~ incubated pyDOM samples.

~~The observed diversity of bio-produced formulas can be explained by a scenario wherein the microbes secreted labile molecules whose identities differed depending on the growth medium and/or food source, yielding high variability among bio-produced formulas after the incubation of pyDOM. Additionally, it is possible that different microbial species (different bacteria, fungi, archaea, etc.) have proliferated in response to the sample-specific pyDOM composition, yielding different microbial populations growing during each different incubation, sequentially producing different bio-produced compounds (Fitch et al., 2018). Another possible explanation for the observed diversification is the presence of ROS-driven oxygenation processes. ROS are known to be key species in the consumption of organic matter by microbes. Microbes can only consume small molecules that could pass through their cell membranes (Sinsabaugh et al., 1997; Fuchs et al., 2011; Burns et al., 2013). Thus, to utilize large molecules as food, microbes produce exoenzymes which generate ROS extracellularly (Hyde and Wood, 1997; Higuchi, 2004). These ROS then degrade the large molecules into smaller ones that are utilized as food. Though not directly proven to exist in this study, many of the observed trends in FT-ICR-MS, NMR, and fluorescence data suggest the presence of radicals which diversify the composition of the bio-produced formulas.~~

~~The observed diversity can be explained by a scenario wherein the microbes secreted labile molecules whose identities differed depending on the growth medium and/or food source, yielding high variability among bio-produced formulas after the incubation of pyDOM. Additionally, it is possible that different microbial species (different bacteria, fungi, archaea, etc.) have proliferated in response to the sample-specific pyDOM composition, yielding different microbial populations growing during each different incubation, sequentially producing different bio-produced compounds (Fitch et al., 2018).~~

The Our finding of extreme molecular diversity contrasts with previous observations ~~made by Lechtenfeld et al. (2015)~~ in a study by Lechtenfeld et al. (2015) evaluating the molecular composition of microbially produced DOM. In their study, marine microbes were supplied with two different substrates (glucose and glutamic acid; and a mixture of oligosaccharides and oligopeptides), and a significant overlap (67 – 69 %) in the bio-produced organic matter was observed. The difference in observations between the work presented in this manuscript and by Lechtenfeld et al. (2015) is likely caused by a large difference in the composition of the pyDOM substrates relative to those in the Lechtenfeld et al. (2015) study. While the four pyDOM samples used here are highly heterogeneous to one another (Goranov et al., 2020; Wozniak et al., 2020), the substrates by Lechtenfeld et al. (2015) were of much higher similarity (glucose, glutamic acid, oligosaccharides and oligopeptides). Another possible reason is that due to different the physiology ~~of~~ the soil microbes used here may be producing more diverse molecules-biomass than the marine microbes used by Lechtenfeld et al. (2015). It is likely that ~~that~~ aquatic microbes have a much different degradation strategy than soil microbes. As soils are far less rich in labile molecules, it is possible that soil microbes have adapted-evolved to produce much higher fluxes of ROS to degrade the more recalcitrant soil organic matter into consumable substrates, which can also explain the larger dissimilarity in bio-produced organic molecules after the incubations of pyDOM. ~~The observed diversity can be explained by a scenario wherein the microbes secreted labile molecules whose identities differed depending on~~

the growth medium and/or food source, yielding high variability among bio-produced formulas after the incubation of pyDOM. Additionally, it is possible that different microbial species (different bacteria, fungi, archaea, etc.) have proliferated in response to the sample-specific pyDOM composition, yielding different microbial populations growing during each different incubation, sequentially producing different bio-produced compounds (Fitch et al., 2018).

The observations from this study are compared to previous work by Waggoner et al. (2017) where a ligninaceous sample was treated with three different ROS: hydroxyl radical ( $\bullet\text{OH}$ ), singlet oxygen ( $^1\text{O}_2$ ), and superoxide ( $\text{O}_2^-$ ). Each different radical degraded a specific pool of ligninaceous compounds, which showed that different ROS can degrade a variety of types of organic matter. However, there was a significant overlap observed between the three pools of molecules that were degraded indicating that degradation pathways solely based on ROS attacks are still ordered. Thus, because ROS on their own do not produce completely diversified molecular pools, the combination of the two pathways we describe here must have occurred to produce the great variability in the bio-produced microbial biomass observed in our study.

An important observation using the H/C versus molecular weight/MW plots (Fig. S5) was that the bio-produced compounds after incubation of pyDOM were of various molecular weights/MW. Thus, it is likely that that the microbial biomass produced during the incubation is radically coupled with ambient pyDOM molecules or their biochemical remnants. This has Radical coupling been recently proposed as an important process in marine DOM cycling (Hach et al., 2020). In that study, when isotopically  $^{13}\text{C}$ -labeled organisms were incubated with oceanic surface waters, microbially produced compounds were quickly coupled to the ambient marine DOM molecules. This “recombination” process occurred within hours of the production of microbial exudates, followed by the observation of a highly diversified DOM pool. This process is likely driven by radical coupling reactions, and such pathways have also been observed in incubations in the presence of sunlight (Sun et al., 2017). Another possible explanation is that chemically reactive species, such as quinones, reacted with microbially produced compounds or the  $\text{NH}_4^+$  nutrient via nucleophile-driven reactions (such as the Michael addition; McKee et al., 2014) to produce highly diverse pools of molecules after each incubation.

The observations from this study Our results are also compared to previous work by Waggoner et al. (2017) where a ligninaceous sample was treated with three different ROS: hydroxyl radical ( $\bullet\text{OH}$ ), singlet oxygen ( $^1\text{O}_2$ ), and superoxide ( $\text{O}_2^-$ ). Each different radical degraded a specific pool of ligninaceous compounds, which showed that different ROS can degrade a variety of types of organic matter. However, there was a significant overlap observed between the three pools of molecules that were degraded (Waggoner et al., 2017) indicating that degradation pathways solely based on ROS attacks are still ordered. Thus, because ROS on their own do not produce completely diversified molecular pools, the combination of the two possible pathways (consumption and ROS degradation) we describe here must have occurred to produce the great variability in the bio-produced microbial biomass observed in our study.

Collectively, our results indicate that pyDOM can be both directly consumed by biota and secondarily degraded by ROS-driven processes. These pathways could not be explored at a mechanistic level in the current study, and we suggest that future studies focus on employing more specialized analytical techniques (e.g., genetic sequencing, ROS quantification) for deconvoluting the complexity of the bio-degradation of pyDOM. — The observations from this study are compared to previous work by Waggoner et al. (2017) where a ligninaceous sample was treated with three different ROS: hydroxyl radical ( $\bullet\text{OH}$ ), singlet oxygen ( $^1\text{O}_2$ ), and superoxide ( $\text{O}_2^-$ ). Each different radical degraded a specific pool of ligninaceous compounds, which showed that different ROS can degrade a variety of types of organic matter. However, there was a significant overlap observed between the three pools of molecules that were degraded indicating that degradation pathways solely based on ROS attacks are still ordered. Thus, because ROS on their own do not produce completely diversified molecular pools, the combination of the two pathways we describe here must have occurred to produce the great variability in the bio-produced microbial biomass observed in our study.

Clearly, the chemistry behind these microbially induced compositional changes of pyDOM is highly complex, and the observed molecular diversity after these biotic incubations contrasts with previous studies.

877 ~~These discrepancies cannot be interpreted unambiguously using the employed analytical approaches, and future~~  
878 ~~studies need to involve measurements of radicals and their effects, as well as various DNA sequencing and~~  
879 ~~“omics” approaches.~~

## 881 4.2 Implications for the cycling of pyDOM in the environment

882  
883 The present study provides a detailed evaluation of the compounds that microbes degrade and produce in  
884 samples mimicking pyDOM in hydrologically dynamic ~~environmental~~ systems such as riverine and groundwater  
885 systems. ~~This work~~ brings new knowledge ~~about regarding~~ the properties and ~~reactivity degradability~~ of pyDOM  
886 and challenges the conventional idea that pyDOM is stable towards biotic degradation. Several studies have  
887 already shown that pyrogenic substances have soluble DOM components (Hockaday et al., 2007; Mukherjee and  
888 Zimmerman, 2013; Wagner et al., 2017; Bostick et al., 2018) and that more soluble components are produced  
889 with environmental aging (Abiven et al., 2011; Ascough et al., 2011; Roebuck et al., 2017; Quan et al., 2020). ~~A~~  
890 ~~recent study incubated pyDOM using riverine microbes and observed a significant degree of degradation as well~~  
891 ~~(Qi et al., 2020). However, rather than using an extracted inoculate, in that work, the authors directly incubated~~  
892 ~~pyOM in riverine water. Therefore, these incubations can be considered primed by the more labile riverine~~  
893 ~~molecules (Guenet et al., 2010; Bianchi, 2011).~~ The experiments presented ~~in our study here~~, in parallel with  
894 Bostick et al. (~~2020a2021~~), show that a large portion of pyDOM can be ~~respired remineralized~~ (bio-degraded ~~to~~  
895 ~~CO<sub>2</sub>) without priming (Guenet et al., 2010; Bianchi, 2011), which indicates that these pyrogenic molecules may~~  
896 ~~be far less resistant to bio-degradation than previously presumed.~~

897 The involvement of pyDOM within the global carbon cycle is complex, and ~~in many cases for many~~  
898 ~~biogeochemical processes~~, poorly understood. There is a growing body of literature showing that significant  
899 amounts of ~~pyOM ConAC~~ are solubilized and exported to the global ocean (Dittmar et al., 2012; Jaffé et al., 2013;  
900 Wang et al., 2016; Marques et al., 2017; Jones et al., 2020) ~~suggesting constant global leaching of pyDOM in~~  
901 ~~riverine systems from pyOM in soils. The global riverine flux of pyDOM is estimated using the recently reported~~  
902 ~~global flux of ConAC (18 Tg·C·y<sup>-1</sup>) and scaled using a factor of 7.5 as proposed by Bostick et al. (2018) to be~~  
903 ~~135 Tg·C·y<sup>-1</sup>, a value that is much lower than~~ However, the estimated ~~annual~~ pyDOM production and seepage  
904 ~~flux rates~~ of 1440 Tg·C·y<sup>-1</sup> (Bostick et al., 2018) ~~are greater than previously reported riverine flux estimates (203~~  
905 ~~Tg·C·y<sup>-1</sup>; Jaffé et al., 2013; rescaled by Bostick et al., 2018).~~ In addition to the implied ~~8691~~% loss of carbon  
906 during ~~riverine~~ export, a recent study also reported that the stable carbon isotopic signature ( $\delta^{13}\text{C}$ ) of oceanic  
907 ConAC ~~are is~~ not ~~terrigenousterrestrial~~, but rather, marine-like (Wagner et al., 2019). This suggests that either all  
908 ~~of the~~ riverine-exported ConAC are being mineralized before ~~they reaching~~ the global ocean or ~~ConAC~~ are  
909 chemically altered significantly to change ~~its-their~~  $\delta^{13}\text{C}$  isotopic signature (Jones et al., 2020). ~~Furthermore,~~  
910 ~~m~~ Microbial and photochemical processes have been found to transform DOM with characteristic  
911 ~~terrigenousterrestrial~~ DOM composition (compounds with lower H/C and higher O/C ratios) into compounds  
912 having characteristics of marine-derived DOM (compounds with higher H/C, lower O/C ratios; Rossel et al.,  
913 2013). Thus, pyDOM may simply be losing its diagnostic molecular and isotopic ~~terrestrial-like~~ fingerprints  
914 during riverine export due to a variety of degradative post-production processes, ~~as shown by and~~ the  
915 ~~diversification observed molecular transformations observed~~ in our study ~~are likely one of them.~~

916 The cycling of organic matter in the environment has always been an enigma, and there has been a long-  
917 standing effort to explain the fate of ~~land-derived terrestrial~~ DOM (~~terrigenous DOM~~ including pyDOM) in the  
918 global ocean (Hedges et al., 1997). In a previous manuscript evaluating the photochemical transformation of  
919 pyDOM (Goranov et al., 2020), we suggested that biotic consumption of photo-degradation products of pyDOM  
920 (“small aliphatic compounds”) could result in the formation of marine-like DOM. This hypothesis was tested by  
921 comparing our incubation products (the bio-produced formulas) to FT-ICR-MS formulas of ~~an estuarine transect~~  
922 ~~of the Elizabeth River, VA (Sleighter and Hatcher, 2008) and another ten several marine-oceanic~~ DOM samples  
923 (reported in Sect. 5 of the Supplement). ~~An insignificant number of common formulas was CRAM-like marine~~  
924 ~~formulas (Hertkorn et al., 2006) was~~ observed in these comparisons (~~1934 – 272308~~ common formulas, ~~0-8 –~~  
925 ~~618~~% overlap) ~~confirming the hypothesis that bio-incubation of pyDOM can produce marine-like DOM. The~~  
926 ~~observed common formulas were not condensed and 81 – 192 of them (42 – 70%) were of molecular composition~~



927 attributed to carboxyl-rich alicyclic molecules (CRAM) per Hertkorn et al. (2006). These results indicate that  
928 ~~contrasting with this proposition and suggesting that~~ biotic incubations of ~~photo-degraded~~ pyDOM (regardless of  
929 ~~photo-irradiation~~) ~~do not produce significant numbers of~~ can contribute to some of the molecules observed in  
930 ~~oceanic environments, marine-like molecules.~~ The fact that some of these molecules were observed in both  
931 surface and abyssal oceanic DOM indicate that some pyDOM bio-degradation products may be sequestered into  
932 the deep ocean as refractory DOM.

933 The observed bio-produced labile formulas in our study do not appear to be commonly observed in other  
934 environmental samples. This is likely because these labile molecules ~~An alternative idea is that the bio-produced~~  
935 ~~molecules observed in this study~~ are part of the fast-cycling, labile DOM pool per Hansell's model (Hansell and  
936 Carlson, 2015), and are quickly depleted in the natural environment. This parallels the findings of a recently  
937 published study (Hach et al., 2020) observing that microbially produced molecules are extremely labile and are,  
938 within hours, broken down and recombined with ambient DOM molecules. The closed laboratory systems in our  
939 study, may have enabled the observation of these highly labile molecules, whereas in the natural environment,  
940 they would have been quickly transformed, diluted, or mineralized to inorganic carbon resulting in their removal  
941 from analytical detection. The richness in nitrogen and peptide-like character of ~~these the bio-produced~~new  
942 molecules we observe suggest greater potential lability (Hach et al., 2020), and it is likely that the by-products of  
943 biotic degradation of pyDOM are readily incorporated into microbial food webs. This is consistent with the idea  
944 that ~~terrigenousterrestrial~~ DOM is either mineralized to CO<sub>2</sub> or incorporated into food webs (Berggren et al.,  
945 2010a; Ward et al., 2013; Fasching et al., 2014). It is also consistent with the suggestionfact that the majority of  
946 organic nitrogen in the oceans is derived from microbial peptidoglycans (McCarthy et al., 1997, 1998; Simpson  
947 et al., 2011), and with observations of nitrogen from peptidoglycans in soil and sedimentary porewater systems  
948 (Schulten and Schnitzer, 1998; Hu et al., 2018, 2020).

949 The production of ~~these~~ highly variable and diverse bio-produced molecules, ~~compositionally~~, is likely a  
950 contributing factor to the large complexity of natural organic matter (Hertkorn et al., 2007; Hawkes et al., 2018).  
951 ~~They~~Our observed bio-produced molecules likely contribute to the highly variable microbial exometabolomes  
952 observed previously (Antón et al., 2013; Watrous et al., 2013; Romano et al., 2014) and stimulate further questions  
953 about ~~their pyDOM's~~ function and fate within the global carbon and nitrogen cycles. In this study, we have used  
954 soil microbes, as the corresponding degradation by-products can be observed in both soil, groundwater, and  
955 partially in the upstream sections of rivers. Therefore, it would be critical to perform further studies with different  
956 microbial consortia (riverine, estuarine, marine, etc.) to fully understand the biological degradation of pyDOM in  
957 different environments. Additionally, the observed evidence for two possible degradative pathways (consumption  
958 and ROS degradation) indicates that these pyDOM incubations are extremely complex systems. Future  
959 microbiological studies must aim to investigate these pathways further by designing radical quenching  
960 experiments (to test for presence/absence of radical oxygenation pathways) as well as employ bio-analytical  
961 techniques (e.g., genetic sequencing; Nalven et al., 2020) for assessing what microbes are responsible for the  
962 labilization and diversification of pyDOM.

## 964 5 Conclusions

965  
966 This study probing the molecular changes occurring after biotic degradation of pyDOM revealed that soil  
967 microbes can effectively recycle and transform a significant portion of pyDOM molecules into labile microbial  
968 biomass. After the 10-day incubations, it appears that a wide range of pyDOM molecules, both aromatic and  
969 aliphatic, were degraded, forming a highly diverse pool of compounds, including N-containing compounds with  
970 proteinaceous signatures and a peptidoglycan-like backbone. These observations are consistent with the previous  
971 identification of nitrogen from peptidoglycans in soils and oceans. These bio-produced compounds were highly  
972 specific for each pyDOM sample which was concluded by observing (very few common bio-produced molecular  
973 formulas among incubated samples). The observed molecular labilization and diversification have implications  
974 for the studies of for the biogeochemistry of pyDOMwildfire biogeochemistry, as this-we shows that microbial  
975 reworking of pyDOM can contribute to the large complexity and variability of natural organic matter. This study  
976 reveals that 1) pyDOM can be a medium for microbial growth, and 2) previously considered "recalcitrant"



pyrogenic molecules can be broken down and the carbon and nitrogen therein can be incorporated into microbial food webs. This study suggests that pyDOM is a much more active component in the global carbon and nitrogen cycles and that some non-condensed pyDOM degradation products have an oceanic fate. Therefore,–and future studies need to further evaluate the bio-reactivitydegradability of pyDOM with microbial consortia of different environments, as well as in the context of wetted soils, groundwater processes, cycling within the riverine and marine water columns, and other aspects of the global carbon and nitrogen cycles.

*Data Availability.* Research Data associated with this article can be accessed at <https://doi.org/10.17632/kjkhy3tfys.1>

*Competing Interests.* The authors declare that they have no conflict of interest.

*Author Contributions.* Conceptualization, A.I.G, A.S.W., K.W.B., A.R.Z., S.M., P.G.H.; Investigation, K.W.B., A.I.G.; Formal analysis, A.I.G.; Writing – Original Draft Preparation, A.I.G.; Writing – Review & Editing, A.I.G, A.S.W., K.W.B., A.R.Z., S.M., P.G.H.; Funding Acquisition, A.S.W., A.R.Z., S.M., P.G.H.

*Acknowledgments.* We thank Rachel L. Sleighter for providing the marine-estuarine and oceanic FT-ICR-MS data. We also thank Isaiah Ruhl, Dr. Deepti Varma, and Dr. Ravi Garimella for assistance during instrumental analyses at the COSMIC facility (Old Dominion University), and Dow Van Arnam (University of Florida) for design and construction of the biochar pyrolyzer and solar simulator. This project was funded by National Science Foundation (Geobiology and Low-Temperature Geochemistry Program, proposal numbers EAR-1451452 and EAR-1451367) and the Frank Batten Endowment Fund to Dr. Patrick G. Hatcher (Old Dominion University). Additionally, we appreciate Old Dominion University for supporting Aleksandar I. Goranov through the Dominion Fellowship. Lastly, we would like to express our gratitude to the editor and reviewers-referees for their time and feedback in improving this manuscript.

## References

- Abboudi, M., Jeffrey, W. H., Ghiglione, J. F., Pujo-Pay, M., Oriol, L., Sempéré, R., Charrière, B., and Joux, F.: Effects of photochemical transformations of dissolved organic matter on bacterial metabolism and diversity in three contrasting coastal sites in the Northwestern Mediterranean Sea during summer, *Microbial Ecology*, 55, 344-357, <https://doi.org/10.1007/s00248-007-9280-8>, 2008.
- Abiven, S., Hengartner, P., Schneider, M. P. W., Singh, N., and Schmidt, M. W. I.: Pyrogenic carbon soluble fraction is larger and more aromatic in aged charcoal than in fresh charcoal, *Soil Biology & Biochemistry*, 43, 1615-1617, <https://doi.org/10.1016/j.soilbio.2011.03.027>, 2011.
- Antón, J., Lucio, M., Peña, A., Cifuentes, A., Brito-Echeverría, J., Moritz, F., Tziotis, D., López, C., Urdiain, M., Schmitt-Kopplin, P., and Rosselló-Móra, R.: High metabolomic microdiversity within co-occurring isolates of the extremely halophilic bacterium *Salinibacter ruber*, *PLoS ONE*, 8, 1-14, <https://doi.org/10.1371/journal.pone.0064701>, 2013.
- Antony, R., Sanyal, A., Kapse, N., Dhakephalkar, P. K., Thamban, M., and Nair, S.: Microbial communities associated with Antarctic snow pack and their biogeochemical implications, *Microbiological Research*, 192, 192-202, <https://doi.org/10.1016/j.micres.2016.07.004>, 2016.
- Antony, R., Willoughby, A. S., Grannas, A. M., Catanzano, V., Sleighter, R. L., Thamban, M., Hatcher, P. G., and Nair, S.: Molecular insights on dissolved organic matter transformation by supraglacial microbial communities, *Environmental Science & Technology*, 51, 4328-4337, <https://doi.org/10.1021/acs.est.6b05780>, 2017.
- Antony, R., Willoughby, A. S., Grannas, A. M., Catanzano, V., Sleighter, R. L., Thamban, M., and Hatcher, P. G.: Photo-biochemical transformation of dissolved organic matter on the surface of the coastal East Antarctic ice sheet, *Biogeochemistry*, 141, 229-247, <https://doi.org/10.1007/s10533-018-0516-0>, 2018.

- 026 Ascough, P. L., Bird, M. I., Francis, S. M., Thornton, B., Midwood, A. J., Scott, A. C., and Apperley, D.:  
027 Variability in oxidative degradation of charcoal: Influence of production conditions and environmental  
028 exposure, *Geochimica et Cosmochimica Acta*, 75, 2361-2378, <https://doi.org/10.1016/j.gca.2011.02.002>,  
029 2011.
- 030 Bao, H., Niggemann, J., Luo, L., Dittmar, T., and Kao, S.-J.: Aerosols as a source of dissolved black carbon to  
031 the ocean, *Nature Communications*, 8, 1-7, <https://doi.org/10.1038/s41467-017-00437-3>, 2017.
- 032 Bax, A., and Davis, D. G.: MLEV-17-based two-dimensional homonuclear magnetization transfer spectroscopy,  
033 *Journal of Magnetic Resonance*, 65, 355-360, [https://doi.org/10.1016/0022-2364\(85\)90018-6](https://doi.org/10.1016/0022-2364(85)90018-6), 1985.
- 034 Benner, R., and Biddanda, B.: Photochemical transformations of surface and deep marine dissolved organic  
035 matter: Effects on bacterial growth, *Limnology and Oceanography*, 43, 1373-1378,  
036 <https://doi.org/10.4319/lo.1998.43.6.1373>, 1998.
- 037 Berggren, M., Laudon, H., Haei, M., Ström, L., and Jansson, M.: Efficient aquatic bacterial metabolism of  
038 dissolved low-molecular-weight compounds from terrestrial sources, *The ISME Journal*, 4, 408-416,  
039 <https://doi.org/10.1038/ismej.2009.120>, 2010a.
- 040 Berggren, M., Ström, L., Laudon, H., Karlsson, J., Jonsson, A., Giesler, R., Bergström, A.-K., and Jansson, M.:  
041 Lake secondary production fueled by rapid transfer of low molecular weight organic carbon from  
042 terrestrial sources to aquatic consumers, *Ecology Letters*, 13, 870-880, <https://doi.org/10.1111/j.1461-0248.2010.01483.x>, 2010b.
- 044 Bianchi, T. S.: The role of terrestrially derived organic carbon in the coastal ocean: A changing paradigm and the  
045 priming effect, *Proceedings of the National Academy of Sciences of the United States of America*, 108,  
046 19473–19481, <https://doi.org/10.1073/pnas.1017982108>, 2011.
- 047 Billen, G., Servais, P., and Becquevort, S.: Dynamics of bacterioplankton in oligotrophic and eutrophic aquatic  
048 environments: Bottom-up or top-down control?, *Hydrobiologia*, 207, 37-42,  
049 <https://doi.org/10.1007/BF00041438>, 1990.
- 050 Bostick, K. W., Zimmerman, A. R., Wozniak, A. S., Mitra, S., and Hatcher, P. G.: Production and composition  
051 of pyrogenic dissolved organic matter from a logical series of laboratory-generated chars, *Frontiers in*  
052 *Earth Science*, 6, 1-14, <https://doi.org/10.3389/feart.2018.00043>, 2018.
- 053 Bostick, K. W., Zimmerman, A. R., Goranov, A. I., Mitra, S., Hatcher, P. G., and Wozniak, A. S.: Biolability of  
054 fresh and photodegraded pyrogenic dissolved organic matter from laboratory-prepared chars, *Journal of*  
055 *Geophysical Research: Biogeosciences*, 126, 1-17, <https://doi.org/10.1029/2020JG005981>,  
056 2021. ~~Bostick, K. W., Zimmerman, A. R., Goranov, A. I., Mitra, S., Hatcher, P. G., and Wozniak, A. S.:~~  
057 ~~Biolability of fresh and photodegraded pyrogenic dissolved organic matter from laboratory-prepared~~  
058 ~~chars, *ESSOAr [pre-print]*, <https://doi.org/10.1002/essoar.10503766.1>, 31 July 2020.~~
- 059 Bostick, K. W., Zimmerman, A. R., Goranov, A. I., Mitra, S., Hatcher, P. G., and Wozniak, A. S.: Photolability  
060 of pyrogenic dissolved organic matter from a thermal series of laboratory-prepared chars, *Science of The*  
061 *Total Environment*, 724, 1-9, <https://doi.org/10.1016/j.scitotenv.2020.138198>, 2020b.
- 062 Burns, R. G., DeForest, J. L., Marxsen, J., Sinsabaugh, R. L., Stromberger, M. E., Wallenstein, M. D., Weintraub,  
063 M. N., and Zoppini, A.: Soil enzymes in a changing environment: Current knowledge and future  
064 directions, *Soil Biology & Biochemistry*, 58, 216-234, <https://doi.org/10.1016/j.soilbio.2012.11.009>,  
065 2013.
- 066 Chen, M., and Jaffé, R.: Photo- and bio-reactivity patterns of dissolved organic matter from biomass and soil  
067 leachates and surface waters in a subtropical wetland, *Water Research*, 61, 181-190,  
068 <https://doi.org/10.1016/j.watres.2014.03.075>, 2014.
- 069 Chistoserdova, L., Chen, S.-W., Lapidus, A., and Lidstrom, M. E.: Methylotrophy in *Methylobacterium*  
070 *extorquens* AM1 from a genomic point of view, *Journal of Bacteriology*, 185, 2980-2987,  
071 <https://doi.org/10.1128/JB.185.10.2980-2987.2003>, 2003.
- 072 Chistoserdova, L., and Kalyuzhnaya, M. G.: Current trends in methylotrophy, *Trends in Microbiology*, 26, 703-  
073 714, <https://doi.org/10.1016/j.tim.2018.01.011>, 2018.
- 074 Coble, P. G.: Characterization of marine and terrestrial DOM in seawater using excitation-emission matrix  
075 spectroscopy, *Marine Chemistry*, 51, 325-346, [https://doi.org/10.1016/0304-4203\(95\)00062-3](https://doi.org/10.1016/0304-4203(95)00062-3), 1996.

- 076 Coble, P. G., Lead, J., Baker, A., Reynolds, D. M., and Spencer, R. G. M.: Aquatic Organic Matter Fluorescence,  
077 Cambridge University Press, New York, NY, 2014.
- 078 Coppola, A. I., Seidel, M., Ward, N. D., Viviroli, D., Nascimento, G. S., Haghypour, N., Revels, B. N., Abiven,  
079 S., Jones, M. W., Richey, J. E., Eglinton, T. I., Dittmar, T., and Schmidt, M. W. I.: Marked isotopic  
080 variability within and between the Amazon River and marine dissolved black carbon pools, *Nature*  
081 *Communications*, 10, 1-8, <https://doi.org/10.1038/s41467-019-11543-9>, 2019.
- 082 D'Andrilli, J., Fischer, S. J., and Rosario-Ortiz, F. L.: Advancing critical applications of high resolution mass  
083 spectrometry for DOM assessments: Re-engaging with mass spectral principles, limitations, and data  
084 analysis, *Environmental Science & Technology*, 54, 11654-11656,  
085 <https://doi.org/10.1021/acs.est.0c04557>, 2020.
- 086 Dittmar, T., Koch, B., Hertkorn, N., and Kattner, G.: A simple and efficient method for the solid-phase extraction  
087 of dissolved organic matter (SPE-DOM) from seawater, *Limnology and Oceanography: Methods*, 6, 230-  
088 235, <https://doi.org/10.4319/lom.2008.6.230>, 2008.
- 089 Dittmar, T., and Paeng, J.: A heat-induced molecular signature in marine dissolved organic matter, *Nature*  
090 *Geoscience*, 2, 175-179, <https://doi.org/10.1038/ngeo440>, 2009.
- 091 Dittmar, T., de Rezende, C. E., Manecki, M., Niggemann, J., Coelho Ovalle, A. R., Stubbins, A., and Bernardes,  
092 M. C.: Continuous flux of dissolved black carbon from a vanished tropical forest biome, *Nature*  
093 *Geoscience*, 5, 618-622, <https://doi.org/10.1038/ngeo1541>, 2012.
- 094 Druffel, E.: Comments on the importance of black carbon in the global carbon cycle, *Marine Chemistry*, 92, 197-  
095 200, <https://doi.org/10.1016/j.marchem.2004.06.026>, 2004.
- 096 Dyrda, G., Boniewska-Bernacka, E., Man, D., Barchiewicz, K., and Słota, R.: The effect of organic solvents on  
097 selected microorganisms and model liposome membrane, *Molecular Biology Reports*, 46, 3225-3232,  
098 <https://doi.org/10.1007/s11033-019-04782-y>, 2019.
- 099 Fasching, C., Behounek, B., Singer, G. A., and Battin, T. J.: Microbial degradation of terrigenous dissolved  
100 organic matter and potential consequences for carbon cycling in brown-water streams, *Scientific Reports*,  
101 4, 1-7, <https://doi.org/10.1038/srep04981>, 2014.
- 102 Fitch, A., Orland, C., Willer, D., Emilson, E. J. S., and Tanentzap, A. J.: Feasting on terrestrial organic matter:  
103 Dining in a dark lake changes microbial decomposition, *Global change biology*, 24, 5110-5122,  
104 <https://doi.org/10.1111/gcb.14391>, 2018.
- 105 Fu, H. Y., Liu, H. T., Mao, J. D., Chu, W. Y., Li, Q. L., Alvarez, P. J. J., Qu, X. L., and Zhu, D. Q.: Photochemistry  
106 of dissolved black carbon released from biochar: Reactive oxygen species generation and  
107 phototransformation, *Environmental Science & Technology*, 50, 1218-1226,  
108 <https://doi.org/10.1021/acs.est.5b04314>, 2016.
- 109 Fuchs, G., Boll, M., and Heider, J.: Microbial degradation of aromatic compounds - from one strategy to four,  
110 *Nature Reviews Microbiology*, 9, 803-816, <https://doi.org/10.1038/nrmicro2652>, 2011.
- 111 Goldberg, E. D.: Black carbon in the environment: Properties and distribution, J. Wiley, New York, NY, 1985.
- 112 Gonsior, M., Hertkorn, N., Hinman, N., Dvorski, S. E., Harir, M., Cooper, W. J., and Schmitt-Kopplin, P.:  
113 Yellowstone hot springs are organic chemodiversity hot spots, *Scientific Reports*, 8, 1-13,  
114 <https://doi.org/10.1038/s41598-018-32593-x>, 2018.
- 115 Goranov, A. I., Wozniak, A. S., Bostick, K. W., Zimmerman, A. R., Mitra, S., and Hatcher, P. G.: Photochemistry  
116 after fire: Structural transformations of pyrogenic dissolved organic matter elucidated by advanced  
117 analytical techniques, *Geochimica et Cosmochimica Acta*, 290, 271-292,  
118 <https://doi.org/10.1016/j.gca.2020.08.030>, 2020.
- 119 Gottlieb, H. E., Kotlyar, V., and Nudelman, A.: NMR chemical shifts of common laboratory solvents as trace  
120 impurities, *The Journal of Organic Chemistry*, 62, 7512-7515, <https://doi.org/10.1021/Jo971176v>, 1997.
- 121 Green, S. A., and Blough, N. V.: Optical absorption and fluorescence properties of chromophoric dissolved  
122 organic matter in natural waters, *Limnology and Oceanography*, 39, 1903-1916,  
123 <https://doi.org/10.4319/lo.1994.39.8.1903>, 1994.
- 124 Guenet, B., Danger, M., Abbadie, L., and Lacroix, G.: Priming effect: Bridging the gap between terrestrial and  
125 aquatic ecology, *Ecology*, 91, 2850-2861, <https://doi.org/10.1890/09-1968.1>, 2010.

- 126 Gurganus, S. C., Wozniak, A. S., and Hatcher, P. G.: Molecular characteristics of the water soluble organic matter  
127 in size-fractionated aerosols collected over the North Atlantic Ocean, *Marine Chemistry*, 170, 37-48,  
128 <https://doi.org/10.1016/j.marchem.2015.01.007>, 2015.
- 129 Hach, P. F., Marchant, H. K., Krupke, A., Riedel, T., Meier, D. V., Lavik, G., Holtappels, M., Dittmar, T., and  
130 Kuypers, M. M. M.: Rapid microbial diversification of dissolved organic matter in oceanic surface waters  
131 leads to carbon sequestration, *Scientific Reports*, 10, 1-10, <https://doi.org/10.1038/s41598-020-69930-y>,  
132 2020.
- 133 Hansell, D. A., and Carlson, C. A.: *Biogeochemistry of marine dissolved organic matter*, Second ed., Academic  
134 Press, Amsterdam, 712 pp., 2015.
- 135 Hawkes, J. A., Patriarca, C., Sjöberg, P. J. R., Tranvik, L. J., and Bergquist, J.: Extreme isomeric complexity of  
136 dissolved organic matter found across aquatic environments, *Limnology and Oceanography Letters*, 3,  
137 21-30, <https://doi.org/10.1002/lo2.10064>, 2018.
- 138 Hedges, J. I., Keil, R. G., and Benner, R.: What happens to terrestrial organic matter in the ocean?, *Organic*  
139 *Geochemistry*, 27, 195-212, [https://doi.org/10.1016/S0146-6380\(97\)00066-1](https://doi.org/10.1016/S0146-6380(97)00066-1), 1997.
- 140 Helms, J. R., Stubbins, A., Ritchie, J. D., Minor, E. C., Kieber, D. J., and Mopper, K.: Absorption spectral slopes  
141 and slope ratios as indicators of molecular weight, source, and photobleaching of chromophoric dissolved  
142 organic matter, *Limnology and Oceanography*, 53, 955-969, <https://doi.org/10.4319/lo.2008.53.3.0955>,  
143 2008.
- 144 Hemmler, D., Gonsior, M., Powers, L. C., Marshall, J. W., Rychlik, M., Taylor, A. J., and Schmitt-Kopplin, P.:  
145 Simulated sunlight selectively modifies Maillard reaction products in a wide array of chemical reactions,  
146 *Chemistry*, 25, 13208-13217, <https://doi.org/10.1002/chem.201902804>, 2019.
- 147 Hertkorn, N., Benner, R., Frommberger, M., Schmitt-Kopplin, P., Witt, M., Kaiser, K., Kettrup, A., and Hedges,  
148 J. I.: Characterization of a major refractory component of marine dissolved organic matter, *Geochimica*  
149 *et Cosmochimica Acta*, 70, 2990-3010, <https://doi.org/10.1016/j.gca.2006.03.021>, 2006.
- 150 Hertkorn, N., Ruecker, C., Meringer, M., Gugisch, R., Frommberger, M., Perdue, E., Witt, M., and Schmitt-  
151 Kopplin, P.: High-precision frequency measurements: Indispensable tools at the core of the molecular-  
152 level analysis of complex systems, *Analytical and Bioanalytical Chemistry*, 389, 1311-1327,  
153 <https://doi.org/10.1007/s00216-007-1577-4>, 2007.
- 154 Higuchi, T.: Microbial degradation of lignin: Role of lignin peroxidase, manganese peroxidase, and laccase,  
155 *Proceedings of the Japan Academy, Series B*, 80, 204-214, <https://doi.org/10.2183/pjab.80.204>, 2004.
- 156 Hockaday, W. C., Grannas, A. M., Kim, S., and Hatcher, P. G.: Direct molecular evidence for the degradation  
157 and mobility of black carbon in soils from ultrahigh-resolution mass spectral analysis of dissolved organic  
158 matter from a fire-impacted forest soil, *Organic Geochemistry*, 37, 501-510,  
159 <https://doi.org/10.1016/j.orggeochem.2005.11.003>, 2006.
- 160 Hockaday, W. C., Grannas, A. M., Kim, S., and Hatcher, P. G.: The transformation and mobility of charcoal in a  
161 fire-impacted watershed, *Geochimica et Cosmochimica Acta*, 71, 3432-3445,  
162 <https://doi.org/10.1016/j.gca.2007.02.023>, 2007.
- 163 Hockaday, W. C., Purcell, J. M., Marshall, A. G., Baldock, J. A., and Hatcher, P. G.: Electrospray and  
164 photoionization mass spectrometry for the characterization of organic matter in natural waters: A  
165 qualitative assessment, *Limnology and Oceanography: Methods*, 7, 81-95,  
166 <https://doi.org/10.4319/lom.2009.7.81>, 2009.
- 167 Hu, Y., Zheng, Q., Zhang, S., Noll, L., and Wanek, W.: Significant release and microbial utilization of amino  
168 sugars and D-amino acid enantiomers from microbial cell wall decomposition in soils, *Soil Biology &*  
169 *Biochemistry*, 123, 115-125, <https://doi.org/10.1016/j.soilbio.2018.04.024>, 2018.
- 170 Hu, Y., Zheng, Q., Noll, L., Zhang, S., and Wanek, W.: Direct measurement of the *in situ* decomposition of  
171 microbial-derived soil organic matter, *Soil Biology & Biochemistry*, 141, 1-10,  
172 <https://doi.org/10.1016/j.soilbio.2019.107660>, 2020.
- 173 Hughey, C. A., Hendrickson, C. L., Rodgers, R. P., Marshall, A. G., and Qian, K.: Kendrick mass defect spectrum:  
174 a compact visual analysis for ultrahigh-resolution broadband mass spectra, *Analytical Chemistry*, 73,  
175 4676-4681, <https://doi.org/10.1021/ac010560w>, 2001.



- Hyde, S. M., and Wood, P. M.: A mechanism for production of hydroxyl radicals by the brown-rot fungus *Coniophora Puteana*: Fe(III) reduction by cellobiose dehydrogenase and Fe(II) oxidation at a distance from the hyphae, *Microbiology*, 143, 259-266, <https://doi.org/10.1099/00221287-143-1-259>, 1997.
- Idowu, O., Semple, K. T., Ramadass, K., O'Connor, W., Hansbro, P., and Thavamani, P.: Beyond the obvious: Environmental health implications of polar polycyclic aromatic hydrocarbons, *Environ Int*, 123, 543-557, <https://doi.org/10.1016/j.envint.2018.12.051>, 2019.
- Jaffé, R., Ding, Y., Niggemann, J., Vähätalo, A. V., Stubbins, A., Spencer, R. G. M., Campbell, J., and Dittmar, T.: Global charcoal mobilization from soils via dissolution and riverine transport to the oceans, *Science*, 340, 345-347, <https://doi.org/10.1126/science.1231476>, 2013.
- Johns, G: Austin Cary Forest Prescribed Burn (33/8S/21E), School of Forest Resources and Conservation, UF/IFAS, Prescribed Burn Prescription 721, 1-5, 2016
- Jones, M. W., Coppola, A. I., Santín, C., Dittmar, T., Jaffé, R., Doerr, S. H., and Quine, T. A.: Fires prime terrestrial organic carbon for riverine export to the global oceans, *Nature Communications*, 11, 1-8, <https://doi.org/10.1038/s41467-020-16576-z>, 2020.
- Judd, K. E., Crump, B. C., and Kling, G. W.: Bacterial responses in activity and community composition to photo-oxidation of dissolved organic matter from soil and surface waters, *Aquatic Sciences*, 69, 96-107, <https://doi.org/10.1007/s00027-006-0908-4>, 2007.
- Kendrick, E.: A mass scale based on  $\text{CH}_2 = 14.0000$  for high resolution mass spectrometry of organic compounds, *Analytical Chemistry*, 35, 2146-2154, <https://doi.org/10.1021/ac60206a048>, 1963.
- Khatami, S., Deng, Y., Tien, M., and Hatcher, P. G.: Formation of water-soluble organic matter through fungal degradation of lignin, *Organic Geochemistry*, 135, 64-70, <https://doi.org/10.1016/j.orggeochem.2019.06.004>, 2019a.
- Khatami, S., Deng, Y., Tien, M., and Hatcher, P. G.: Lignin contribution to aliphatic constituents of humic acids through fungal degradation, *Journal of Environmental Quality*, 48, 1565-1570, <https://doi.org/10.2134/jeq2019.01.0034>, 2019b.
- Khodadad, C. L. M., Zimmerman, A. R., Green, S. J., Uthandi, S., and Foster, J. S.: Taxa-specific changes in soil microbial community composition induced by pyrogenic carbon amendments, *Soil Biology & Biochemistry*, 43, 385-392, <https://doi.org/10.1016/j.soilbio.2010.11.005>, 2011.
- Kieber, D. J., McDaniel, J., and Mopper, K.: Photochemical source of biological substrates in sea water: Implications for carbon cycling, *Nature*, 341, 637-639, <https://doi.org/10.1038/341637a0>, 1989.
- Kim, S., Kramer, R. W., and Hatcher, P. G.: Graphical method for analysis of ultrahigh-resolution broadband mass spectra of natural organic matter, the van Krevelen diagram, *Analytical Chemistry*, 75, 5336-5344, <https://doi.org/10.1021/ac034415p>, 2003.
- Kirchman, D. L.: Processes in microbial ecology, Second ed., Oxford University Press, 1-318 pp., 2018.
- Klevit, R. E.: Improving two-dimensional NMR spectra by  $t_1$  ridge subtraction, *Journal of Magnetic Resonance*, 62, 551-555, [https://doi.org/10.1016/0022-2364\(85\)90227-6](https://doi.org/10.1016/0022-2364(85)90227-6), 1985.
- Koch, B. P., and Dittmar, T.: From mass to structure: An aromaticity index for high-resolution mass data of natural organic matter, *Rapid Communications in Mass Spectrometry*, 20, 926-932, <https://doi.org/10.1002/rcm.2386>, 2006.
- Koch, B. P., Dittmar, T., Witt, M., and Kattner, G.: Fundamentals of molecular formula assignment to ultrahigh resolution mass data of natural organic matter, *Analytical Chemistry*, 79, 1758-1763, <https://doi.org/10.1021/ac061949s>, 2007.
- Koch, B. P., and Dittmar, T.: From mass to structure: An aromaticity index for high-resolution mass data of natural organic matter (Erratum), *Rapid Communications in Mass Spectrometry*, 30, 1, <https://doi.org/10.1002/rcm.7433>, 2016.
- Kolb, S., and Stacheter, A.: Prerequisites for amplicon pyrosequencing of microbial methanol utilizers in the environment, *Front Microbiol*, 4, 1-12, <https://doi.org/10.3389/fmicb.2013.00268>, 2013.
- Kothawala, D. N., Murphy, K. R., Stedmon, C. A., Weyhenmeyer, G. A., and Tranvik, L. J.: Inner filter correction of dissolved organic matter fluorescence, *Limnology and Oceanography: Methods*, 11, 616-630, <https://doi.org/10.4319/lom.2013.11.616>, 2013.

- 226 Kujawinski, E. B., and Behn, M. D.: Automated analysis of electrospray ionization Fourier transform ion  
227 cyclotron resonance mass spectra of natural organic matter, *Analytical Chemistry*, 78, 4363-4373,  
228 <https://doi.org/10.1021/ac0600306>, 2006.
- 229 Kuzyakov, Y., Subbotina, I., Chen, H., Bogomolova, I., and Xu, X.: Black carbon decomposition and  
230 incorporation into soil microbial biomass estimated by  $^{14}\text{C}$  labeling, *Soil Biology & Biochemistry*, 41,  
231 210-219, <https://doi.org/10.1016/j.soilbio.2008.10.016>, 2009.
- 232 Kuzyakov, Y., Bogomolova, I., and Glaser, B.: Biochar stability in soil: Decomposition during eight years and  
233 transformation as assessed by compound-specific  $^{14}\text{C}$  analysis, *Soil Biology & Biochemistry*, 70, 229-  
234 236, <https://doi.org/10.1016/j.soilbio.2013.12.021>, 2014.
- 235 Lechtenfeld, O. J., Hertkorn, N., Shen, Y., Witt, M., and Benner, R.: Marine sequestration of carbon in bacterial  
236 metabolites, *Nature Communications*, 6, 1-8, <https://doi.org/10.1038/ncomms7711>, 2015.
- 237 Lehmann, J.: A handful of carbon, *Nature*, 447, 143-144, <https://doi.org/10.1038/447143a>, 2007.
- 238 Li, M., Bao, F., Zhang, Y., Sheng, H., Chen, C., and Zhao, J.: Photochemical aging of soot in the aqueous phase:  
239 Release of dissolved black carbon and the formation of  $^1\text{O}_2$ , *Environmental Science & Technology*, 53,  
240 12311-12319, <https://doi.org/10.1021/acs.est.9b02773>, 2019.
- 241 Lindell, M. J., Granéli, W., and Tranvik, L. J.: Enhanced bacterial growth in response to photochemical  
242 transformation of dissolved organic matter, *Limnology and Oceanography*, 40, 195-199,  
243 <https://doi.org/10.4319/lo.1995.40.1.0195>, 1995.
- 244 Liu, M., Mao, X.-a., Ye, C., Huang, H., Nicholson, J. K., and Lindon, J. C.: Improved WATERGATE pulse  
245 sequences for solvent suppression in NMR spectroscopy, *Journal of Magnetic Resonance*, 132, 125-129,  
246 <https://doi.org/10.1006/jmre.1998.1405>, 1998.
- 247 Marques, J. S. J., Dittmar, T., Niggemann, J., Almeida, M. G., Gomez-Saez, G. V., and Rezende, C. E.: Dissolved  
248 black carbon in the headwaters-to-ocean continuum of Paraíba Do Sul River, Brazil, *Frontiers in Earth  
249 Science*, 5, 1-12, <https://doi.org/10.3389/feart.2017.00011>, 2017.
- 250 Masiello, C. A., and Druffel, E. R. M.: Black carbon in deep-sea sediments, *Science*, 280, 1911-1913,  
251 <https://doi.org/10.1126/science.280.5371.1911>, 1998.
- 252 Masiello, C. A.: New directions in black carbon organic geochemistry, *Marine Chemistry*, 92, 201-213,  
253 <https://doi.org/10.1016/j.marchem.2004.06.043>, 2004.
- 254 McCarthy, M., Pratum, T., Hedges, J., and Benner, R.: Chemical composition of dissolved organic nitrogen in  
255 the ocean, *Nature*, 390, 150-154, <https://doi.org/10.1038/36535>, 1997.
- 256 McCarthy, M. D., Hedges, J. I., and Benner, R.: Major bacterial contribution to marine dissolved organic nitrogen,  
257 *Science*, 281, 231-234, <https://doi.org/10.1126/science.281.5374.231>, 1998.
- 258 McKee, G. A., Kobiela, M. E., and Hatcher, P. G.: Effect of Michael adduction on peptide preservation in natural waters,  
259 *Environmental Science: Processes & Impacts*, 16, 2087-2097, [10.1039/C4EM00075G](https://doi.org/10.1039/C4EM00075G), 2014.
- 260 McNally, A. M., Moody, E. C., and McNeill, K.: Kinetics and mechanism of the sensitized photodegradation of  
261 lignin model compounds, *Photochem. Photobiol. Sci.*, 4, 268-274, <https://doi.org/10.1039/b416956e>,  
262 2005.
- 263 Miller, M. P., Simone, B. E., McKnight, D. M., Cory, R. M., Williams, M. W., and Boyer, E. W.: New light on a  
264 dark subject: Comment, *Aquatic Sciences*, 72, 269-275, <https://doi.org/10.1007/s00027-010-0130-2>,  
265 2010.
- 266 Moran, M. A., and Covert, J. S.: Photochemically mediated linkages between dissolved organic matter and  
267 bacterioplankton, in: *Aquatic Ecosystems*, edited by: Findlay, S. E. G., and Sinsabaugh, R. L., Academic  
268 Press, Burlington, 243-262, 2003.
- 269 Moran, M. A., Kujawinski, E. B., Stubbins, A., Fatland, R., Aluwihare, L. I., Buchan, A., Crump, B. C.,  
270 Dorrestein, P. C., Dyhrman, S. T., Hess, N. J., Howe, B., Longnecker, K., Medeiros, P. M., Niggemann,  
271 J., Obernosterer, I., Repeta, D. J., and Waldbauer, J. R.: Deciphering ocean carbon in a changing world,  
272 *Proceedings of the National Academy of Sciences of the United States of America*, 113, 3143-3151,  
273 [10.1073/pnas.1514645113](https://doi.org/10.1073/pnas.1514645113), 2016.

- 274 Múčka, V., Bláha, P., Čuba, V., and Červenák, J.: Influence of various scavengers of •OH radicals on the radiation  
275 sensitivity of yeast and bacteria, *International Journal of Radiation Biology*, 89, 1045-1052,  
276 <https://doi.org/10.3109/09553002.2013.817702>, 2013.
- 277 Mukherjee, A., Zimmerman, A. R., and Harris, W.: Surface chemistry variations among a series of laboratory-  
278 produced biochars, *Geoderma*, 163, 247-255, <https://doi.org/10.1016/j.geoderma.2011.04.021>, 2011.
- 279 Mukherjee, A., and Zimmerman, A. R.: Organic carbon and nutrient release from a range of laboratory-produced  
280 biochars and biochar-soil mixtures, *Geoderma*, 193-194, 122-130,  
281 <https://doi.org/10.1016/j.geoderma.2012.10.002>, 2013.
- 282 Murphy, K. R., Butler, K. D., Spencer, R. G. M., Stedmon, C. A., Boehme, J. R., and Aiken, G. R.: Measurement  
283 of dissolved organic matter fluorescence in aquatic environments: An interlaboratory comparison,  
284 *Environmental Science & Technology*, 44, 9405-9412, <https://doi.org/10.1021/es102362t>, 2010.
- 285 Murphy, K. R.: A note on determining the extent of the water Raman peak in fluorescence spectroscopy, *Applied*  
286 *Spectroscopy*, 65, 233-236, <https://doi.org/10.1366/10-06136>, 2011.
- 287 Murphy, K. R., Stedmon, C. A., Graeber, D., and Bro, R.: Fluorescence spectroscopy and multi-way techniques.  
288 PARAFAC, *Analytical Methods*, 5, 6541-6882, <https://doi.org/10.1039/c3ay41160e>, 2013.
- 289 Nalven, S. G., Ward, C. P., Payet, J. P., Cory, R. M., Kling, G. W., Sharpton, T. J., Sullivan, C. M., and Crump,  
290 B. C.: Experimental metatranscriptomics reveals the costs and benefits of dissolved organic matter photo-  
291 alteration for freshwater microbes, *Environmental Microbiology*, 22, 3505-3521,  
292 <https://doi.org/10.1111/1462-2920.15121>, 2020.
- 293 Obernosterer, I., and Benner, R.: Competition between biological and photochemical processes in the  
294 mineralization of dissolved organic carbon, *Limnology and Oceanography*, 49, 117-124,  
295 <https://doi.org/10.4319/lo.2004.49.1.0117>, 2004.
- 296 Patriarca, C., Balderrama, A., Može, M., Sjöberg, P. J. R., Bergquist, J., Tranvik, L. J., and Hawkes, J. A.:  
297 Investigating the ionization of dissolved organic matter by electrospray ionization, *Analytical Chemistry*,  
298 92, 14210-14218, <https://doi.org/10.1021/acs.analchem.0c03438>, 2020.
- 299 [Patriarca, C., Sedano-Núñez, V. T., Garcia, S. L., Bergquist, J., Bertilsson, S., Sjöberg, P. J. R., Tranvik, L. J.,](#)  
300 [and Hawkes, J. A.: Character and environmental lability of cyanobacteria-derived dissolved organic](#)  
301 [matter, \*Limnology and Oceanography\*, 66, 496-509, https://doi.org/10.1002/lno.11619, 2021.](#)
- 302 Porcal, P., Dillon, P. J., and Molot, L. A.: Photochemical production and decomposition of particulate organic  
303 carbon in a freshwater stream, *Aquatic Sciences*, 75, 469-482, [https://doi.org/10.1007/s00027-013-0293-](https://doi.org/10.1007/s00027-013-0293-8)  
304 8, 2013.
- 305 Powers, L. C., Hertkorn, N., McDonald, N., Schmitt-Kopplin, P., Del Vecchio, R., Blough, N. V., and Gonsior,  
306 M.: *Sargassum sp.* act as a large regional source of marine dissolved organic carbon and polyphenols,  
307 *Global Biogeochemical Cycles*, 33, 1423-1439, <https://doi.org/10.1029/2019GB006225>, 2019.
- 308 Qi, Y., Fu, W., Tian, J., Luo, C., Shan, S., Sun, S., Ren, P., Zhang, H., Liu, J., Zhang, X., and Wang, X.: Dissolved  
309 black carbon is not likely a significant refractory organic carbon pool in rivers and oceans, *Nature*  
310 *Communications*, 11, 1-11, <https://doi.org/10.1038/s41467-020-18808-8>, 2020.
- 311 Qualls, R. G., and Richardson, C. J.: Factors controlling concentration, export, and decomposition of dissolved  
312 organic nutrients in the Everglades of Florida, *Biogeochemistry*, 62, 197-229,  
313 <https://doi.org/10.1023/A:1021150503664>, 2003.
- 314 Quan, G., Fan, Q., Zimmerman, A. R., Sun, J., Cui, L., Wang, H., Gao, B., and Yan, J.: Effects of laboratory  
315 biotic aging on the characteristics of biochar and its water-soluble organic products, *Journal of Hazardous*  
316 *Materials*, 382, 1-9, <https://doi.org/10.1016/j.jhazmat.2019.121071>, 2020.
- 317 Reisser, M., Purves, R. S., Schmidt, M. W. I., and Abiven, S.: Pyrogenic carbon in soils: A literature-based  
318 inventory and a global estimation of its content in soil organic carbon and stocks, *Frontiers in Earth*  
319 *Science*, 4, 1-14, <https://doi.org/10.3389/feart.2016.00080>, 2016.
- 320 Riedel, T., Zark, M., Vähätalo, A. V., Niggemann, J., Spencer, R. G. M., Hernes, P. J., and Dittmar, T.: Molecular  
321 signatures of biogeochemical transformations in dissolved organic matter from ten world rivers, *Frontiers*  
322 *in Earth Science*, 4, 1-16, <https://doi.org/10.3389/feart.2016.00085>, 2016.

- 323 Roebuck, J. A., Podgorksi, D. C., Wagner, S., and Jaffé, R.: Photodissolution of charcoal and fire-impacted soil  
324 as a potential source of dissolved black carbon in aquatic environments, *Organic Geochemistry*, 112, 16-  
325 21, <https://doi.org/10.1016/j.orggeochem.2017.06.018>, 2017.
- 326 Romano, S., Dittmar, T., Bondarev, V., Weber, R. J. M., Viant, M. R., and Schulz-Vogt, H. N.: Exo-metabolome  
327 of *Pseudovibrio sp.* FO-BEG1 analyzed by ultra-high resolution mass spectrometry and the effect of  
328 phosphate limitation, *PLoS ONE*, 9, 1-11, <https://doi.org/10.1371/journal.pone.0096038>, 2014.
- 329 Rossel, P. E., Vähätalo, A. V., Witt, M., and Dittmar, T.: Molecular composition of dissolved organic matter from  
330 a wetland plant (*Juncus effusus*) after photochemical and microbial decomposition (1.25 yr): Common  
331 features with deep sea dissolved organic matter, *Organic Geochemistry*, 60, 62-71,  
332 <https://doi.org/10.1016/j.orggeochem.2013.04.013>, 2013.
- 333 Santín, C., Doerr, S. H., Preston, C. M., and Gonzalez-Rodriguez, G.: Pyrogenic organic matter production from  
334 wildfires: A missing sink in the global carbon cycle, *Global change biology*, 21, 1621-1633,  
335 <https://doi.org/10.1111/gcb.12800>, 2015.
- 336 Santín, C., Doerr, S. H., Merino, A., Bryant, R., and Loader, N. J.: Forest floor chemical transformations in a  
337 boreal forest fire and their correlations with temperature and heating duration, *Geoderma*, 264, 71-80,  
338 <https://doi.org/10.1016/j.geoderma.2015.09.021>, 2016.
- 339 Santín, C., Doerr, S. H., Merino, A., Bucheli, T. D., Bryant, R., Ascough, P., Gao, X., and Masiello, C. A.: Carbon  
340 sequestration potential and physicochemical properties differ between wildfire charcoals and slow-  
341 pyrolysis biochars, *Scientific Reports*, 7, 1-11, <https://doi.org/10.1038/s41598-017-10455-2>, 2017.
- 342 Schmidt, M. W. I., and Noack, A. G.: Black carbon in soils and sediments: Analysis, distribution, implications,  
343 and current challenges, *Global Biogeochemical Cycles*, 14, 777-793,  
344 <https://doi.org/10.1029/1999GB001208>, 2000.
- 345 Schneider, M. P. W., Hilf, M., Vogt, U. F., and Schmidt, M. W. I.: The benzene polycarboxylic acid (BPCA)  
346 pattern of wood pyrolyzed between 200 °C and 1000 °C, *Organic Geochemistry*, 41, 1082-1088,  
347 <https://doi.org/10.1016/j.orggeochem.2010.07.001>, 2010.
- 348 Schulten, H. R., and Schnitzer, M.: The chemistry of soil organic nitrogen: A review, *Biology and fertility of*  
349 *soils*, 26, 1-15, <https://doi.org/10.1007/s003740050335>, 1998.
- 350 Scully, N. M., Cooper, W. J., and Tranvik, L. J.: Photochemical effects on microbial activity in natural waters:  
351 The interaction of reactive oxygen species and dissolved organic matter, *FEMS Microbiology Ecology*,  
352 46, 353-357, [https://doi.org/10.1016/s0168-6496\(03\)00198-3](https://doi.org/10.1016/s0168-6496(03)00198-3), 2003.
- 353 Simpson, A. J., McNally, D. J., and Simpson, M. J.: NMR spectroscopy in environmental research: From  
354 molecular interactions to global processes, *Progress in Nuclear Magnetic Resonance Spectroscopy*, 58,  
355 97-175, <https://doi.org/10.1016/j.pnmrs.2010.09.001>, 2011.
- 356 Sinsabaugh, R. L., Findlay, S., Franchini, P., and Fischer, D.: Enzymatic analysis of riverine bacterioplankton  
357 production, *Limnology and Oceanography*, 42, 29-38, <https://doi.org/10.4319/lo.1997.42.1.0029>, 1997.
- 358 Skjemstad, J., Reicosky, D. C., Wilts, A., and McGowan, J.: Charcoal carbon in U.S. agricultural soils, *Soil*  
359 *Science Society of America Journal*, 66, 1249-1255, <https://doi.org/10.2136/sssaj2002.1249>, 2002.
- 360 Sleighter, R. L., and Hatcher, P. G.: Molecular characterization of dissolved organic matter (DOM) along a river  
361 to ocean transect of the lower Chesapeake Bay by ultrahigh resolution electrospray ionization Fourier  
362 transform ion cyclotron resonance mass spectrometry, *Marine Chemistry*, 110, 140-152,  
363 10.1016/j.marchem.2008.04.008, 2008.
- 364 Sleighter, R. L., McKee, G. A., Liu, Z., and Hatcher, P. G.: Naturally present fatty acids as internal calibrants for  
365 Fourier transform mass spectra of dissolved organic matter, *Limnology and Oceanography: Methods*, 6,  
366 246-253, <https://doi.org/10.4319/lom.2008.6.246>, 2008.
- 367 Sleighter, R. L., Chen, H., Wozniak, A. S., Willoughby, A. S., Caricasole, P., and Hatcher, P. G.: Establishing a  
368 measure of reproducibility of ultrahigh-resolution mass spectra for complex mixtures of natural organic  
369 matter, *Analytical Chemistry*, 84, 9184-9191, <https://doi.org/10.1021/ac3018026>, 2012.
- 370 Smith, C. R., Hatcher, P. G., Kumar, S., and Lee, J. W.: Investigation into the sources of biochar water-soluble  
371 organic compounds and their potential toxicity on aquatic microorganisms, *ACS Sustainable Chemistry*  
372 *& Engineering*, 4, 2550-2558, <https://doi.org/10.1021/acssuschemeng.5b01687>, 2016.



373 Søndergaard, M., and Middelboe, M.: A cross-system analysis of labile dissolved organic carbon, *Marine Ecology*  
374 *Progress Series*, 118, 283-294, <https://doi.org/10.3354/meps118283>, 1995.

375 Spence, A., Simpson, A. J., McNally, D. J., Moran, B. W., McCaul, M. V., Hart, K., Paull, B., and Kelleher, B.  
376 P.: The degradation characteristics of microbial biomass in soil, *Geochimica et Cosmochimica Acta*, 75,  
377 2571-2581, <https://doi.org/10.1016/j.gca.2011.03.012>, 2011.

378 Stenson, A. C., William, M., Marshall, A. G., and Cooper, W. T.: Ionization and fragmentation of humic  
379 substances in electrospray ionization Fourier transform-ion cyclotron resonance mass spectrometry,  
380 *Analytical Chemistry*, 74, 4397-4409, 2002.

381 Stubbins, A., Spencer, R. G. M., Chen, H. M., Hatcher, P. G., Mopper, K., Hernes, P. J., Mwamba, V. L.,  
382 Mangangu, A. M., Wabakanghanzi, J. N., and Six, J.: Illuminated darkness: Molecular signatures of  
383 Congo River dissolved organic matter and its photochemical alteration as revealed by ultrahigh precision  
384 mass spectrometry, *Limnology and Oceanography*, 55, 1467-1477, 10.4319/lo.2010.55.4.1467, 2010.

385 Stubbins, A., Niggemann, J., and Dittmar, T.: Photo-lability of deep ocean dissolved black carbon,  
386 *Biogeosciences*, 9, 1661-1670, <https://doi.org/10.5194/bg-9-1661-2012>, 2012.

387 Sun, L., Xu, C., Zhang, S., Lin, P., Schwehr, K. A., Quigg, A., Chiu, M.-H., Chin, W.-C., and Santschi, P. H.:  
388 Light-induced aggregation of microbial exopolymeric substances, *Chemosphere*, 181, 675-681,  
389 <https://doi.org/10.1016/j.chemosphere.2017.04.099>, 2017.

390 Trusiak, A., Treibergs, L., Kling, G., and Cory, R.: The controls of iron and oxygen on hydroxyl radical ( $\bullet\text{OH}$ )  
391 production in soils, *Soil Systems*, 3, 1-23, <https://doi.org/10.3390/soilsystems3010001>, 2018.

392 Valle, J., Harir, M., Gonsior, M., Enrich-Prast, A., Schmitt-Kopplin, P., Bastviken, D., and Hertkorn, N.:  
393 Molecular differences between water column and sediment pore water SPE-DOM in ten Swedish boreal  
394 lakes, *Water Research*, 170, 1-11, <https://doi.org/10.1016/j.watres.2019.115320>, 2020.

395 Van Krevelen, D. W.: Graphical-statistical method for the study of structure and reaction processes of coal, *Fuel*  
396 *Processing Technology*, 29, 269-228, 1950.

397 Vollmer, W., Blanot, D., and De Pedro, M. A.: Peptidoglycan structure and architecture, *FEMS Microbiology*  
398 *Reviews*, 32, 149-167, <https://doi.org/10.1111/j.1574-6976.2007.00094.x>, 2008.

399 Vorobev, A., Sharma, S., Yu, M., Lee, J., Washington, B. J., Whitman, W. B., Ballantyne, F. t., Medeiros, P. M.,  
400 and Moran, M. A.: Identifying labile DOM components in a coastal ocean through depleted bacterial  
401 transcripts and chemical signals, *Environmental Microbiology*, 20, 3012-3030,  
402 <https://doi.org/10.1111/1462-2920.14344>, 2018.

403 Waggoner, D. C., Chen, H., Willoughby, A. S., and Hatcher, P. G.: Formation of black carbon-like and alicyclic  
404 aliphatic compounds by hydroxyl radical initiated degradation of lignin, *Organic Geochemistry*, 82, 69-  
405 76, <https://doi.org/10.1016/j.orggeochem.2015.02.007>, 2015.

406 Waggoner, D. C., and Hatcher, P. G.: Hydroxyl radical alteration of HPLC fractionated lignin: Formation of new  
407 compounds from terrestrial organic matter, *Organic Geochemistry*, 113, 315-325,  
408 <https://doi.org/10.1016/j.orggeochem.2017.07.011>, 2017.

409 Waggoner, D. C., Wozniak, A. S., Cory, R. M., and Hatcher, P. G.: The role of reactive oxygen species in the  
410 degradation of lignin derived dissolved organic matter, *Geochimica et Cosmochimica Acta*, 208, 171-184,  
411 <https://doi.org/10.1016/j.gca.2017.03.036>, 2017.

412 Wagner, S., and Jaffé, R.: Effect of photodegradation on molecular size distribution and quality of dissolved black  
413 carbon, *Organic Geochemistry*, 86, 1-4, <https://doi.org/10.1016/j.orggeochem.2015.05.005>, 2015.

414 Wagner, S., Ding, Y., and Jaffé, R.: A new perspective on the apparent solubility of dissolved black carbon,  
415 *Frontiers in Earth Science*, 5, 1-16, <https://doi.org/10.3389/feart.2017.00075>, 2017.

416 Wagner, S., Jaffé, R., and Stubbins, A.: Dissolved black carbon in aquatic ecosystems, *Limnology and*  
417 *Oceanography Letters*, 3, 168-185, <https://doi.org/10.1002/lo12.10076>, 2018.

418 Wagner, S., Brandes, J., Spencer, R. G. M., Ma, K., Rosengard, S. Z., Moura, J. M. S., and Stubbins, A.: Isotopic  
419 composition of oceanic dissolved black carbon reveals non-riverine source, *Nature Communications*, 10,  
420 1-8, <https://doi.org/10.1038/s41467-019-13111-7>, 2019.

- 421 Wang, H., Zhou, H., Ma, J., Nie, J., Yan, S., and Song, W.: Triplet photochemistry of dissolved black carbon and  
422 its effects on the photochemical formation of reactive oxygen species, *Environmental Science &*  
423 *Technology*, 54, 4903-4911, <https://doi.org/10.1021/acs.est.0c00061>, 2020.
- 424 Wang, X., Xu, C., Druffel, E. M., Xue, Y., and Qi, Y.: Two black carbon pools transported by the Changjiang  
425 and Huanghe Rivers in China, *Global Biogeochemical Cycles*, 30, 1778-1790,  
426 <https://doi.org/10.1002/2016GB005509>, 2016.
- 427 Ward, C. P., Sleighter, R. L., Hatcher, P. G., and Cory, R. M.: Insights into the complete and partial  
428 photooxidation of black carbon in surface waters, *Environmental Science: Processes & Impacts*, 16, 721-  
429 731, <https://doi.org/10.1039/C3EM00597F>, 2014.
- 430 Ward, N. D., Keil, R. G., Medeiros, P. M., Brito, D. C., Cunha, A. C., Dittmar, T., Yager, P. L., Krusche, A. V.,  
431 and Richey, J. E.: Degradation of terrestrially derived macromolecules in the Amazon River, *Nature*  
432 *Geoscience*, 6, 530-533, <https://doi.org/10.1038/ngeo1817>, 2013.
- 433 Watrous, J., Roach, P., Heath, B., Alexandrov, T., Laskin, J., and Dorrestein, P. C.: Metabolic profiling directly  
434 from the Petri dish using nanospray desorption electrospray ionization imaging mass spectrometry,  
435 *Analytical Chemistry*, 85, 10385-10391, <https://doi.org/10.1021/ac4023154>, 2013.
- 436 Weishaar, J. L., Aiken, G. R., Bergamaschi, B. A., Fram, M. S., Fujii, R., and Mopper, K.: Evaluation of specific  
437 ultraviolet absorbance as an indicator of the chemical composition and reactivity of dissolved organic  
438 carbon, *Environmental Science & Technology*, 37, 4702-4708, <https://doi.org/10.1021/es030360x>, 2003.
- 439 Wetzel, R. G., Hatcher, P. G., and Bianchi, T. S.: Natural photolysis by ultraviolet irradiance of recalcitrant  
440 dissolved organic matter to simple substrates for rapid bacterial metabolism, *Limnology and*  
441 *Oceanography*, 40, 1369-1380, <https://doi.org/10.4319/lo.1995.40.8.1369>, 1995.
- 442 Wienhausen, G., Noriega-Ortega, B. E., Niggemann, J., Dittmar, T., and Simon, M.: The exometabolome of two  
443 model strains of the *Roseobacter* group: A marketplace of microbial metabolites, *Front Microbiol*, 8, 1-  
444 15, <https://doi.org/10.3389/fmicb.2017.01985>, 2017.
- 445 Wozniak, A., Bauer, J., Sleighter, R., Dickhut, R., and Hatcher, P.: Technical note: Molecular characterization of  
446 aerosol-derived water soluble organic carbon using ultrahigh resolution electrospray ionization Fourier  
447 transform ion cyclotron resonance mass spectrometry, *Atmospheric Chemistry and Physics*, 8, 5099-5111,  
448 <https://doi.org/10.5194/acp-8-5099-2008>, 2008.
- 449 Wozniak, A. S., Goranov, A. I., Mitra, S., Bostick, K. W., Zimmerman, A. R., Schlesinger, D. R., Myneni, S.,  
450 and Hatcher, P. G.: Molecular heterogeneity in pyrogenic dissolved organic matter from a thermal series  
451 of oak and grass chars, *Organic Geochemistry*, 148, 1-18,  
452 <https://doi.org/10.1016/j.orggeochem.2020.104065>, 2020.
- 453 Wünsch, U. J., Bro, R., Stedmon, C. A., Wenig, P., and Murphy, K. R.: Emerging patterns in the global  
454 distribution of dissolved organic matter fluorescence, *Analytical Methods*, 11, 888-893,  
455 <https://doi.org/10.1039/C8AY02422G>, 2019.
- 456 Xiao, Y., Carena, L., Näsi, M.-T., and Vähätalo, A. V.: Superoxide-driven autocatalytic dark production of  
457 hydroxyl radicals in the presence of complexes of natural dissolved organic matter and iron, *Water*  
458 *Research*, 1-8, <https://doi.org/10.1016/j.watres.2020.115782>, 2020.
- 459 Yavitt, J. B., and Fahey, T. J.: An experimental analysis of solution chemistry in a lodgepole pine forest floor,  
460 *Oikos*, 43, 222-234, <https://doi.org/10.2307/3544772>, 1984.
- 461 Zeng, Y., Hong, P. K. A., and Wavrek, D. A.: Chemical-biological treatment of pyrene, *Water Research*, 34,  
462 1157-1172, [https://doi.org/10.1016/S0043-1354\(99\)00270-5](https://doi.org/10.1016/S0043-1354(99)00270-5), 2000a.
- 463 Zeng, Y., Hong, P. K. A., and Wavrek, D. A.: Integrated chemical-biological treatment of benzo[a]pyrene,  
464 *Environmental Science & Technology*, 34, 854-862, <https://doi.org/10.1021/es990817w>, 2000b.
- 465 Zimmerman, A. R.: Abiotic and microbial oxidation of laboratory-produced black carbon (biochar),  
466 *Environmental Science & Technology*, 44, 1295-1301, <https://doi.org/10.1021/es903140c>, 2010.
- 467 Zimmerman, A. R., Gao, B., and Ahn, M.-Y.: Positive and negative carbon mineralization priming effects among  
468 a variety of biochar-amended soils, *Soil Biology & Biochemistry*, 43, 1169-1179,  
469 <https://doi.org/10.1016/j.soilbio.2011.02.005>, 2011.